This manuscript is a preprint and has been formally accepted for publication in
Basin Research

Base-Salt Relief Controls Salt-Related Deformation in the Outer Kwanza Basin, offshore Angola

Sian L. Evans*, Christopher A.-L. Jackson

Basins Research Group (BRG), Department of Earth Science & Engineering, Imperial College, Prince Consort Road, London, SW72BP, United Kingdom

*sian.evans15@imperial.ac.uk

Abstract

Salt-influenced passive margins are widespread and commonly hydrocarbon-rich. However, they can be structurally complex, with their kinematic development being poorly understood. Classic models of salt tectonics divide such margins into updip extensional, mid-slope translational, and downdip contractional kinematic domains. Furthermore the faults, folds, and salt walls associated with each kinematic domain are typically assumed to form perpendicular to the maximum principal stress, which in gravitationally driven systems means broadly perpendicular to base salt dip. We use high-resolution 3D seismic reflection data from the Outer Kwanza Basin, offshore Angola to show that these models cannot explain the diversity of salt structures developing on passive margins, especially those defined by considerable relief on the base-of-salt surface.

Overburden seismic-stratigraphic patterns record the basinward translation and rotation, allowing us to reconstruct the origin and evolution of the salt structures. We show structures in the transitional domain of the Outer Kwanza Basin display three dominant trends, each characterised by different structural styles: i) salt walls perpendicular to the overall base salt dip, ii) salt walls parallel to the base salt dip, and iii) salt walls oblique to the base salt dip.

We show that each set of walls has a unique history, with synchronous phases of extension and compression occurring in adjacent structures despite their close spatial relationship. Our analysis suggests that, in the Outer Kwanza Basin, the structural evolution of the salt and overburden is predominantly controlled by translation over relief on the base-salt surface formed above fault scarps associated with a preceding phase of rifting.

Changes in the downdip volumetric flux and velocity of the salt over topographic features can cause local extension or contraction of the salt and its overburden, associated with local acceleration or deceleration of the salt, respectively. This interaction with base-salt relief creates locally variable stress fields that deform the salt and its overburden, overprinting the broader, margin-scale salt tectonics typically associated with gravity gliding and spreading.

1 Introduction

1.1 Passive margin salt-tectonics

There are two end-member models of gravity-driven salt tectonics on passive margins; ‘gravity gliding’, which occurs due to seaward tilting of the margin during continental uplift and basin subsidence, and ‘gravity spreading’, which occurs due to differential loading of the margin, principally by subsalt sediments eroded and shed from the rising continent (Jackson et al., 1994; Schultz-Ela, 2001; Fort et al. 2004; Hudec and Jackson, 2004; Brun and Fort, 2011; Peel, 2014). Salt-influenced passive margins dominated by gravity gliding (e.g. offshore Israel, eastern Mediterranean) are typically divided into broad, kinematically-linked zones of updip extension, mid-slope translation and downdip contraction (Figure 1)). Each zone is associated with a distinct suite of structures within the salt and its overburden. The updip extensional zone is commonly associated with salt-detached normal faults, salt rollers, rafts, graben and turtles, whereas the downdip contractional zone is associated with salt-cored anticlines and thrusts (Brun and Fort, 2011). In both zones, the long-axes of these structures are subparallel to the strike of the margin, reflecting their formation perpendicular to the maximum principal stress, which is aligned in the direction of the base-salt dip.

Similar structures and trends characterize margins dominated by gravity-spreading (e.g. Nile Delta, eastern Mediterranean), which are also divided into kinematic zones of lateral extension within the proximal part of the load and contraction near the distal pinchout of the load. However, in these cases the orientation of the extensional and contractional structures will be determined by the geometry of the load. For example, in the case of a delta prograding out into a basin containing salt, the fold-and-thrust belt will be arcuate, thus mimicking the arcuate geometry of the delta front (Figure 1). Both the gravity gliding and spreading models typically envisage a smoothly seaward-dipping base-salt, despite the fact that many salt basins formed above substantial, pre- or syn-depositional structural relief (e.g. Rowan, 2012; Dooley et al., 2017; Dooley et al. 2018).

1.2 Influence of Base-Salt Relief on Gravity-Driven Deformation

Over geological timescales, the rheological behaviour of salt can be approximated as highly viscous fluid (Weijermars et al., 1993). Fluids such as these are responsive to the geometry of the surface they flow across, and since salt can be deposited shortly after rifting, the base-salt surface is commonly rugose at varying scales (e.g. Hudec et al. 2013). Physical and numerical analogue models, as well as observations from seismically imaged passive margins, show that gravity gliding and the otherwise free seaward flow of salt may be complicated by residual topography on the base-salt surface. Underlying fault scarps or folds can both create an uneven base-salt surface with which the salt interacts as it flows basinward.

For example, Gaullier et al. (1993) use physical analogue models to simulate salt flow over base-salt steps related to relict syn-rift fault scarps. Base-salt steps oblique to the overall gliding direction generate oblique faults in the overburden, demonstrating a strong correlation between structural trends below the salt décollement and those in the overburden. Cobbold and Szatmari (1991) and Tadeu dos Reis et al. (2008) also use physical models, in the latter case supported by natural examples from the western Mediterranean Gulf of Lion, to show how local changes in the base-salt dip direction can locally redirect salt flow. More specifically, they show that convex and concave base-salt surfaces can generate bi-directional or radial gliding patterns. Concave geometries lead to convergent salt flow that can generate compressional structures, whereas convex geometries lead to divergent salt flow that can generate extensional structures.

More recently, Dooley et al. (2017) (see also Dooley et al., 2018) further investigate salt flow over downflow- and upflow-facing steps in the base-salt, showing that the change in salt flux over a step can be associated with local acceleration and deceleration (Figure 2). The ratio of initial salt thickness to the height of step is important as this controls the change in flux across the step, and the contribution of basal drag is greater for thin salt (Figure 2b and 2d) vs. thick salt (Figure 2a and 2c). In the case of a downflow-facing step, these spatial changes in salt flux can generate an extensional hinge at the top of the step, and a contractional hinge at the base (Figure 2d). Further complexity arises when we consider that local stress fields may vary through time as a function of the net seaward salt flow. For example, Dooley et al. (2017) show that as salt contracts at the top of an upflow-facing ramp (Figure 2b), it thickens and gradually allows the salt velocity to increase, which results in overburden extension. However, the reactive or passive diapir that forms in this position may then be squeezed as it translates seaward and later passes through the contractional hinge of another step. Salt structures and their overburden may thus go through multiple phases of extension and contraction, with these local changes in stress fields overprinting the margin-scale kinematic zones associated with classic models of gravity gliding and spreading (Dooley et al. 2018) (Figure 1). These studies show the significant impact base-salt relief can have on the structural evolution of salt-influenced passive margins. More specifically, they show that extension and contraction can occur anywhere on a passive margin, and that structures may develop oblique to the regional dip, more closely mimicking the trend of features on the base-salt surface which influence their growth. There are, however, relatively few natural examples showing how base salt relief can control salt flow and supra-salt deformation patterns.

High-quality 3D seismic reflection data from the Kwanza Basin, offshore Angola, provides us with an opportunity to assess the salt-tectonic development of an area defined by significant base-salt relief. We first characterize the large-scale structure and kinematics of the study area, before focusing in on the development of individual structures during basinward translation of the salt and its overburden. By analysing and interpreting structural and stratigraphic relationships in the overburden, we are able to reconstruct the origin and growth of salt structures. In doing so, we highlight the important role of base-salt relief in controlling the patterns and products of salt flow during passive margin development, and the overall structural evolution of the basin. These data support the observations from physical models discussed above that the widely accepted and applied gravity gliding/spreading models envisaging broad, margin-scale kinematic zones (Figure 1) do not fully capture the variety of structural styles and orientations of salt structures present on many salt-influenced passive margins. Although based on observations from the Kwanza Basin, the implications of the study are likely applicable to other salt-influenced basins and passive margins defined by significant base-salt relief.

2 Geological setting

The Kwanza Basin forms part of the salt-influenced passive margin characterising much of offshore Angola (Evans, 1978). The basin is >300 km wide, stretching from onshore exposures in the Precambrian Congo Craton westwards to the abyssal plain (Hudec and Jackson, 2004). The southern margin of the basin is marked by a line of seamounts and volcanic rocks that separate the Kwanza Basin from the Benguela Basin. The northern margin of the basin is poorly defined, with the Kwanza Basin passing gradually into the Lower Congo Basin.

Rifting of the Kwanza Basin initiated in the Early Cretaceous, associated with the opening of the South Atlantic Ocean during breakup of the supercontinent Gondwana (Brice et al., 1982). A thick layer (locally up to 4 km; Hudec and Jackson, 2004) of Aptian salt was deposited shortly after rifting, draping the residual syn-rift relief. The salt was deposited in two sub-basins separated by a margin-parallel chain of platforms, known as the Atlantic hinge zone, where salt is thin or absent (Figure 3b) (Brink, 1974; Hudec and Jackson, 2004). The sub-basins are termed the Inner (eastern and landward) and Outer (western and seaward) Kwanza Basins. Analogous salt basins are present across the Atlantic on the conjugate South American margin (Evans, 1978; Quirk et al., 2012).

Since the deposition of the Aptian salt, salt tectonics have dominated the tectono-stratigraphic evolution of the Kwanza Basin (Marton et al., 2000). Hudec and Jackson (2004) interpreted key structures on a regional 2D seismic line, and defined the updip extensional and downdip contractional domains (Figure 3a, location shown in Figure 4). They restored the section shown in Figure 3, and used this restoration to describe three principal phases of salt-related deformation in the Kwanza Basin. First, an early Albian phase of gravity gliding initiated shortly after salt deposition, as the margin tilted during post-rift thermal subsidence. The rate of gravity gliding slowed in the late Albian due to thinning of the salt beneath the updip extensional domain. Second, a phase of rejuvenated salt tectonics occurred in the Campanian, linked to crustal uplift in the distal basin. During this phase the Angola salt nappe was expelled seaward above the distal ramp and onto newly emplaced oceanic crust. Finally, in the Miocene, the rate of downslope translation increased once more as the basin slope (and base-salt) steepened in response to continental uplift. Due to these phases of salt-related deformation, the Kwanza Basin is now characterised by a diverse range of salt-related structures associated with complex suprasalt deformation patterns (Duval et al., 1992; Lundin, 1992; Spathopoulos, 1996; Peel et al., 1998; Marton et al., 2000; Jackson et al., 2001; Hudec and Jackson, 2002; Fort et al., 2004; Hudec and Jackson, 2004; Quirk et al., 2012).

In terms of the regional structural framework established by Hudec and Jackson (2004), the study area falls within the intermediate domain between pure updip extension and pure downdip contraction (i.e. the relatively undeformed zone of pure translation is lacking cf. Figure 1a) (Figure 3). Hudec and Jackson (2004) refer to this area as the 'monocline' and 'diapir' domains. The monocline domain is characterised by subhorizontal or landward-dipping packages of sediments that terminate against prominent onlap surfaces. The diapir domain is characterised by a diverse variety of salt structures including salt-cored anticlines, salt rollers, stocks, walls and allochthonous sheets. The salt structures and associated stratigraphic packages imaged within the study area will be described and interpreted in Sections 4 and 5.

3 Data and Methods

We use a 3D seismic cube, acquired by CGG, covering a broadly rectangular area of 2915 km^2 offshore Angola (Figure 4). The Pre-Stack Depth Migrated (PSDM) BroadSeis™ data are excellent quality and image down to the base-salt, which lies up to 5.5 km below the seabed. The data are zero phase and normal polarity, with a downward increase in acoustic impedance (e.g. top salt) defined by a positive/negative reflection (i.e. blue/red on displayed seismic profiles). The vertical and horizontal resolution are approximated by a quarter of the dominant wavelength of the data, yielding c. 3.5 m (λ=14 m) at the seabed and c. 30 m (λ=120 m) at a depth of 5 km (Brown, 2011).

We mapped several key horizons across the dataset; these were selected based on their regional significance (i.e. truncation marking an unconformity, or change in seismic character inferred to mark a significant lithological boundary). The mapped surfaces show the present basin geometry. These surfaces are used to calculate isopachs that show the distribution and evolution of sedimentary depocentres through time, and which we primarily relate to salt-driven deformation and related changes in accommodation. A lack of available well data means that lithologies and absolute ages are unconstrained. However, in order to approximate horizontal translation rates, Top Albian, Top Eocene and Top Miocene ages are tentatively assigned based on a correlation with surfaces and units published by Hudec and Jackson (2004). Note, however, that we focus primarily on the *relative* timing of events based on seismic-stratigraphic analysis, rather than the *absolute* timing with regards to the regional tectono-stratigraphic framework.

4 Basin Structure

4.1 Base-Salt

The base-salt surface (Figure 5a) dips dominantly to the SW with an average dip of 7°, although we observe significant local changes in both dip and dip direction. The most striking feature is the NW-trending, SW-dipping ramp across the eastern, updip edge of the study area (Figure 5a; see also Figure 6). The ramp, presumed to be a degraded relict fault scarp, formed during the earlier rifting phase (Figure 3a; see also Hudec and Jackson, 2004) and has c. 1.3 km of relief and an average dip of 12°. In detail, despite being broadly perpendicular to the base-salt dip direction, the ramp trend changes along strike. Furthermore, some segments of the ramp, in plan-view, have a convex-, whereas others have a concave-, towards-the-basin geometry. We also note several sub-circular, isolated base-salt highs (Figure 5a).

4.2 Salt Thickness

The salt isopach map (Figure 5b) shows the distribution of salt structures across the study area. These structures display a wide range of orientations and geometries, with no clear systematic pattern to their spatial distribution. The salt structures, in addition to displaying different trends across the study area, vary in structural style (e.g Figure 6). For example, some are associated with normal faults and salt rollers, whereas others are spatially related to thrust faults and buckle folds. We provide a detailed description of these salt structures, and their relationship to the base-salt geometry and overburden structures in Section 6.

4.3 Overburden

We map four main supra-salt seismic-stratigraphic units (Figure 8a-d; corresponding to units highlighted in Figure 6). The thickness map for Unit 1, which broadly equates to the Albian interval, is the most uniform, showing a gradual increase in thickness to the south-east (from c. 400 to c. 1200 m) (Figure 8a). The unit is absent where it has been subsequently pierced by the underlying salt (e.g. Figure 6), but unlike the overlying units, there are only minor and local, salt-related thickness changes, on the order of c. 200-300m).

By comparison, the thickness patterns for Units 2-4 (Figure 8b-d) are considerably more complex. Of particular note are the prominent, NNE-to-NNW-trending depocentres visible in all three isopachs, where the unit thickness increases from c. 500 m to >1500 m over a relatively short (<5 km) length scale. These depocentres contain stacked packages of landward-thickening and dipping strata that onlap or downlap their immediately underlying units (Figure 6). These are the same packages of landward-dipping strata identified by Hudec and Jackson (2004) in their monocline domain (see Section 2). We describe and interpret the origin of these complex overburden thickness patterns below (Section 5).

5 Basin-scale Kinematics

We interpret that the landward-thickening and -dipping packages described in Section 4.3 (Figure 6) form a series of stacked ‘ramp-syncline basins’ (RSBs) that developed in response to the progressive downdip translation of the salt and its overburden across the major base-salt ramp located along the updip edge of the study area (Figure 5a) (Peel et al., 1998; Marton et al., 1998; Jackson et al., 2001; Jackson and Hudec, 2005; Dooley et al., 2017; Pichel et al., 2018; Dooley et al., 2018; Pichel et al., 2019). A RSB is defined as a “translating growth syncline that gradually moves seaward on a dipping detachment as if on a conveyor belt” by Hudec and Jackson (2017). Translation over the seaward-dipping ramp continually creates accommodation on the downdip side of the ramp, causing syn-kinematic strata to thicken landward into the ramp (Figure 7). As displacement continues, strata are rotated downward such that primary onlap relationships now appear as downlap relationships. The RSBs are therefore recognised by their characteristic pseudo-downlap surface and monoclinal geometry of the growth strata (Jackson and Hudec, 2005). Similar examples have previously been described on the Angolan margin using 2D seismic data (Peel et al., 1998; Marton et al., 1998; Jackson et al., 2001; Jackson and Hudec, 2005), and using 3D data from the conjugate margin in the Santos Basin, offshore Brazil (Pichel et al. 2018). RSBs have also been produced in physical analogue models (Dooley et al., 2017; Dooley et al., 2018) and numerical models (Pichel et al., 2018) (Figure 7).

We interpret that the RSBs imaged in the dataset are genetically related to the base-salt ramp located immediately updip (Fig. 5a). Given that each RSB forms at the same position above the major base-salt ramp and is subsequently translated seaward as salt flow progresses, we can reconstruct the overburden translation through time by mapping-out the sedimentary depocentres and their onlaps, and laterally restoring them to their initial positions adjacent to the ramp. The lowermost, and thus earliest, onlap onto the base of each RSB is laterally restored to its original position above the updip hinge of the ramp (Figure 6), and the associated depocentres are fitted as closely as possible to their (inferred) original positions directly overlying the ramp (Figure 8e-g), as shown by physical and numerical models (Dooley et al., 2017; Dooley et al., 2018; Pichel et al., 2018). This process is relatively straightforward for the large, elongate

RSB depocentres, hence their original positions are quite well-constrained. However, it is more difficult to restore the original positions of the smaller, more rounded, yet clearly RSB-related depocentres located in the NW of the study area (Figure 8e-g). We therefore focus the discussion here on the N-trending, linear RSBs for which we can make a confident restoration. The approximate original positions of the smaller depocentres use the vectors and displacement magnitudes given by the larger RSBs to guide their restorations.

The earliest onlap contained within the RSB defines the net distance of translation (Pichel et al., 2018). Our analysis shows that the oldest RSB, RSB 1, records 23.2 km of seaward translation, and 32° of clockwise rotation from its original position to its present day position (Figure 8e). Note that this is a minimum estimate of the total horizontal translation, as it does *not* include any translation that may have occurred during the Albian, prior to the development of the RSB. Our estimate does, however, broadly agree with the estimate of Hudec and Jackson (2004), who calculated at least 20 km of lateral translation based on their structural restoration. We infer the earliest onlap surface is approximately end Albian in age (see Section 3), which equates to 23.2 km of lateral translation in 100.5 Ma (i.e. from the end of the Albian to the present). This yields an average translation rate of c. 0.23 mm/yr, and an average rotation rate of 0.3°/Myr. Previous translation estimates using RSBs used 2D seismic sections and were therefore unable to determine any syn-translation rotation; we think this is the first time this phenomenon has been quantified from a salt basin. Plan-view rotation of salt structures associated with salt flow over base-salt relief has been suggested from analysis of seismic reflection data in the Santos Basin, offshore Brazil (Pichel et al., 2019), and documented in physical models (Dooley and Hudec, 2017).

RSB 2 overlies RSB 1 (Figure 6), and is now located c. 11.3 km seaward from, and has rotated clockwise 12° from, its causal ramp (Figure 8f), whereas the youngest, RSB 3, is located 5.4 km seaward of the ramp and has undergone 5° of clockwise rotation (Figure 8g). If we apply the approximate ages to these units (see Section 3), we can estimate the incremental change in rates of translation and rotation through time (Table 1).

This analysis suggests that translation and rotation rates were approximately constant from the end of the Albian up to the Miocene, at which point they both increased (see Figure 9, in which 10% error bars shown for each data point), an observation is consistent with a previous study by Hudec and Jackson (2004). Translation rates are usually highest during the initial stages of salt tectonics, and decrease through time due to salt thinning and overburden thickening (Jackson and Hudec, 2005). However, in the case of the Kwanza Basin, basement uplift during the Miocene steepened the bathymetric gradient and greatly accelerated downslope translation during the latter stages of margin development (Hudec and Jackson, 2004). Due to the relatively poor age constraints within strata filling the RSBs, we cannot resolve shorter periods of acceleration or deceleration that may have occurred. Rather, our values are broad averages of the rates of translation and rotation for each time step.

The RSBs show that the dominant direction of translation is westward, oblique to the dominant, broadly south-westerly base-salt dip direction (Figure 5a). Clockwise rotation of the RSBs may be explained by variations in the depositional thickness of underlying salt. Due to reduced basal drag, areas of thick salt (in the south) would flow faster seaward than areas of thin salt (in the north), thereby causing a net-clockwise rotation of the translating overburden (Jackson and Hudec, 2017). Von Nicolai (2011) used backstripping and isostatic balancing to determine the initial distribution of salt deposited during the Aptian, showing early local thickness changes that suggest the original salt isopach thickened to the south in this area (see her Figure 4.11).

Having used the RSBs to interpret and quantify the net overburden translation and rotation associated with salt flow in the region of interest, we now proceed with a seismic-stratigraphic analysis of the individual salt structures. Given that we now know how these structures have moved through time from their original positions on the margin, we can interpret their evolution in the context of this basinward translation and their interaction with base-salt relief.

While we are confident applying these translation and rotation estimates to the evolution of local salt structures, we would caution against applying these more widely. A series of thick-skinned transfer faults, which run perpendicular to the margin and segment the Kwanza Basin, are said to allow different amounts of translation on either side of the faults (Duval et al., 1992;

Spathopoulos, 1996). This could mean that the rates of translation and rotation calculated here may only apply locally and may differ along the margin.

6 Local Salt Structure Evolution in the Context of Regional Salt Flow

The salt structures can be grouped into three broad sets defined by their orientations (Figure 5c): (i) Set 1 - Parallel to margin (NW-SE); (ii) Set 2 - Perpendicular to margin (NE-SW); and (iii) Set 3 - Oblique to margin (N-S). Each of these sets is also associated with distinctly different structural styles (e.g. salt rollers and turtle structures vs. thrusts and buckle folds). In a classic gravity gliding-dominated view of salt-influenced passive margins, we might expect elongate salt-related structures (i.e. faults, folds and walls) to be oriented subparallel to the margin (Bally, 1981). As we demonstrate below, the trend and styles of salt structures in this part of the Kwanza Basin deviate from this view, suggesting other processes, such as salt flow over base-salt relief, controlled the structural development of the salt and its overburden. In the following section we describe and interpret the characteristic structural styles of each of the sets, and explore how the base-salt relief may have influenced their structural development during seaward translation.

6.1 Set 1: Margin-Parallel Salt Structures

6.1.1 Geometry and seismic-stratigraphy

There are two NW-trending, margin-parallel salt walls, oriented perpendicular to the general base-salt dip direction and oblique to the dominant (westerly) gliding direction (Figure 5c). The major base-salt ramp is located c. 15 km updip of, and is subparallel to, these two walls. Both salt walls have a broadly triangular shape in cross section, defined by a wide base and narrow crest, and share similar structural characteristics, but the more northerly structure is significantly larger (Figure 10a). Furthermore, the structural characteristics of the larger wall (Figure 10a) vary along strike. Near the centre, the wall has rounded crests, and is flanked by more steeply dipping strata that only onlap the wall in their upper part (Figure 11a). In contrast, at its end, the wall has lower relief and an irregular crestal geometry defined by ‘horn-like’ projections of salt (Figure 11b). In this location, two large, inward-dipping, salt-detached normal faults bound a supra-wall graben.

Unit 1 is broadly tabular, terminating against the salt wall on both flanks (Figure 10a). However, strata at the base of Unit 1 are folded, with growth strata preserved within synclines (Figure 10b). The folds and related growth strata are draped by more tabular, largely deformed strata. Unit 2, however, thins onto both flanks of the salt wall, and forms part of the fill of RSB 1 on the updip side of the structure (Figure 10a). Unit 3 marks a significant change in structural style as it thickens across a series of inward-dipping, graben-defining normal faults developed above the salt wall (Figure 10a). Updip, Unit 3 thickens into a salt-detached normal fault located above the major base-salt ramp. Unit 4 is also faulted over the crest of the salt wall, but overall thickens updip into RSB 3.

6.1.2 Structural Evolution

Based on the geometry and seismic-stratigraphy of the overburden, the structural evolution of the Set 1 salt walls, and their relation to the updip RSB, is summarised here and illustrated schematically in Figure 12.

The presence of growth strata shows that the buckle folds formed during deposition of Unit 1, implying salt-related deformation initiated when the overburden was very thin (only c. 0.1 km thick, based on the thickness of the tabular strata underlying the growth strata; Figure 10b). Our earlier analysis of the RSBs showed that a significant amount (at least c. 23 km) of basinward translation has occurred in the area. We therefore propose that this very early contractional deformation may reflect overburden shortening at the base of the ramp as salt flowed seaward (Figure 2d) (e.g. Dooley et al., 2017; 2018). As a result, the thin overburden buckled to form low-amplitude, small-wavelength folds at the base of the ramp (Figure 12a; Figure 17a). The buckle folds were subsequently translated further downdip to their present position. These kinematics and related structural style are analogous to the translated fold-belt of prekinematic strata generated in a physical model by Dooley et al. (2017) (see their Figure 25).

Thinning of Unit 2 onto the large salt wall indicates that it had a topographic expression on the seafloor during deposition. The associated buckle folds suggest a possible contractional origin for the diapiric structure, which may have initially formed as a salt-cored anticline (Figure 12b; Figure 17b). An alternative interpretation is that the structure formed at the extensional hinge at the top of the ramp (Figure 2d), but we favor the contractional origin because buckle folds of similar age occur on the updip flank of the structure. Once the initial anticline had formed, subsidence of strata immediately flanking the walls occurred as salt was drawn into the core of the growing structure. Sediment loading would have then amplified this effect and driven continued growth of the structure as it translated basinward.

Following continued sediment deposition, the overburden reached a critical thickness where it became too strong to buckle at the base of the ramp. The buckle folds and salt-cored anticlines were thus passively translated downdip as gliding continued, and a RSB formed above the ramp due to an imbalance in salt flux (Figure 12c). The RSB is essentially the expression of the hinge pair/monocline as the roof thickens and strengthens.

A phase of extension, possibly related to salt acceleration as the margin steepened and base-salt dip increased, then caused two graben to develop. One graben developed over the crest of the salt-cored anticline where the overburden was thin and therefore mechanically weak, whereas the other formed over the extensional hinge of the ramp where the stress is greatest (Figure 12d). Overburden extension initiated reactive diapiric rise and allowed the salt to penetrate to the seafloor (Vendeville and Jackson, 1992a) (Figure 17c).

As the diapir rose reactively and drew in more salt, the seaward-dipping, graben-bounding fault above the ramp became dominant, growing and detaching into the salt (Figure 12e). Normal displacement on the fault facilitated the downslope transport of material in this location (Figure 12f), laterally equivalent to RSB 2 developing along strike to the SE. Eventually, diapir growth slowed and it became buried, as the source layer thinned and almost welded (Figure 12g).

Following reactive rise, the salt wall was tall enough, and the overburden thin enough, to permit active rise by buoyancy in the centre of the salt wall. The diapir assumed a more rounded geometry characteristic of active rise in this location (Jackson and Hudec, 2017) (Figure 11a; Figure 17d). In order to feed the actively rising central diapir, salt flowed along-strike from its ends, causing the ends of the salt wall to collapse/fall (Vendeville and Jackson, 1992b) (Figure 11b). The diapir welded on its north-eastern margin, and only a thin connection to the adjacent salt pillow on the south-western edge remains (Figure 10a), thus salt flowed more easily within the salt wall itself. Onlapping strata in the youngest package indicate active rise may be ongoing, although the lack of topographic expression on the present seafloor suggests that either the sediment accumulation rate keeps pace with the rate of diapir rise, or that the active rise has very recently ceased (Figure 17e).

6.2 Set 2: Margin-Perpendicular Salt Structures

6.2.1 Geometry and Seismic Stratigraphy

The NE-trending salt walls are oriented perpendicular to the margin and parallel to the general base-salt dip (Figure 5c). These walls have strikingly different structural characteristics to Set 1 (Figure 13). For example, in contrast to walls defining Set 1, which are broad and normal faulted across the crest, walls in Set 2 are short and narrow, each being associated with a thrust fault that detaches in the crest of the structure (Figure 13a). The predominantly SE-dipping thrust faults are confined to Units 1 and 2, terminating at the contact between Units 2 and 3.

Unit 1 comprises a series of discrete rafts, within which strata thicken to the south-east (Figure 13a). Unit 2 overlies Unit 1 conformably and fills depocentres between detached blocks of Unit 1. Locally, Unit 2 strata define antiformal 'turtle' structures filled with growth strata (Figure 13b). Unit 3 drapes the salt walls and intervening depocentres unconformably, and overlying units are undeformed. Strata at the base of Unit 4 appear to downlap Unit 3; this relationship arises because Figure 13a represents an oblique, NW-trending section through a broadly N-trending RSB. Of particular note in Unit 3 is the broad anticline directly above a topographic high on the base-salt surface; we return to the significance of this structure below.

6.2.2 Structural Evolution

The schematic structural evolution of the Set 2 salt walls is shown in Figure 14. We propose that these salt walls initiated in response to a phase of early extension, which was accommodated by formation of predominantly W-dipping normal faults and associated salt rollers (that later evolved into walls; Figure 14a; Figure 17a). Continued extension eventually dissected Unit 1 into a series of detached rafts, with Unit 2 filling the accommodation between the rafts as the salt thinned (Figure 14b; Figure 17b). An extensional turtle structure formed out-of-plane to the NE

(Figure 13b), similar to asymmetric turtle structures previously been identified in the Kwanza Basin (Duval et al., 1992).

Using the translation and rotation increments given by the RSBs (Section 5), we can restore the original position of the structures. This shows that the Set 2 structures initially formed outside of the area imaged in our seismic data (Fig. 17a). It is therefore difficult to suggest a mechanism for the extension that triggered salt roller formation. However, based on the magnitude of rotation recoded in the RSBs, we can infer that Set 2 structures originally trended broadly N (Fig. 17a), before being rotated into their present NE trend (Fig. 17e). Furthermore, the dominant (restored; see Fig. 17a) westward dip direction of the normal faults bounding the rollers and rafts suggests formation in response to bulk westward sliding. We therefore tentatively infer that the base-salt dips locally to the west (rather than south-westwards) where the Set 2 structures originated. This would be in line with the regional gliding direction indicated by the RSBs, and consistent with observations of roller and raft development elsewhere (e.g. Duval et al., 1992).

The contact between Units 2 and 3 defines the onset of contraction; this exploited the pre-existing planes of weakness created by the salt rollers, which were relatively weaker than the flanking rafts (Figure 14c; Figure 17c). Note that the thrust faults dip to the SE and cross-cut the oppositely dipping, salt-detached, raft-bounding normal faults, likely because the latter were too steep to be reactivated in a reverse sense. The thrust faults uplifted strata above the salt rollers, which were then locally eroded prior to deposition of Unit 3.

The bulk (i.e. regional) shortening direction responsible for squeezing and inversion the Set 2 structures is difficult to determine given contraction exploited pre-existing, weak salt rollers; i.e. the maximum principal stress may have been oblique, rather than perpendicular, to the orientation of the salt walls (Duffy et al., 2018). At the onset of shortening the structures would have been approaching a concave-into-the-basin ramp segment (Figure 17c). Local contraction at this time may therefore relate to the onset of convergent radial gliding associated with translation over this concave-into-the-basin ramp (Cobbold and Szatmari, 1991; Tadeu dos Reis et al, 2008).

From the deposition of Unit 3 onward, there is little evidence of salt-related deformation, with Unit 3 draping and burying the established salt walls (Figure 14d; Figure 17d). The broad fold defined at the top of Unit 3, and associated thinning of Unit 4 above the base-salt high, formed as the overburden was folded during overall basinward translation across base-salt relief (Figure 14f).

6.3 Set 3: Oblique Salt Structures

6.3.1 Geometry and Seismic Stratigraphy

The N-trending salt structures are (presently) oriented oblique to the general base-salt dip direction, perpendicular to the dominant (westerly) gliding direction (see Section 5), and parallel to the RSBs. Unlike those in sets 1 and 2, most of the structures in Set 3 are high-amplitude salt-cored anticlines that do not pierce the overlying stratigraphy (i.e. they are not diapirs; Hudec and Jackson, 2011) (Figure 15). There is one exception that has pierced the overburden and penetrates close to the present day sea floor (furthest west in Figure 15). Unit 1 is largely isopachous across the salt-cored anticlines, whereas Unit 2 thins over the crests and thickens dramatically into flanking synclines (Figure 15). Unit 3 onlaps the salt-cored topographic highs, whereas Unit 4 does not markedly changed in thickness across the underlying salt structures.

6.3.2 Structural Evolution

The stratigraphic occurrence of growth strata indicates that Set 3 salt structures had a rapid and short-lived phase of growth during deposition of Unit 2. This is in contrast to Sets 1 and 2, which formed early during deposition of Unit 1. Set 3 salt structures also differ from Sets 1 and 2 in that they do not show diagnostic characteristics associated with either compression or extension. For example, salt-cored anticlines in Set 3 may have formed as – 1) halokinetic folds, in response to sedimentary loading in the absence of lateral tectonic forces, or 2) contractional folds, in response to lateral compressive forces. Halokinetic folds typically form gradually and are associated with low-relief salt pillows or anticlines, whereas the short-wavelength and tight geometry of these folds, in addition to their relatively rapid growth, is perhaps most consistent with a compressive origin (Jackson and Hudec, 2017).

The schematic structural evolution of the Set 3 salt structures is shown in Figure 16. The N-trending salt-cored anticlines are parallel to the N-trending axes of the RSBs and the N-trending segment of the base-salt ramp responsible for their development (Figure 5a). It therefore follows that the compression that generated the folds and salt pillows was also associated with a deceleration during translation across the base-salt ramp. Decelerating flow at the base of the N-trending ramp could have generated the compressive stress in the same way described for the early buckle folds in Section 6.1, but since the amplitude and wavelength of the folds is proportional to the overburden thickness, the folds generated in this case were larger (see Price and Cosgrove, 1990). Downdip welding during this time may also have served to enhance the deceleration and salt accumulation, though the timing of welding is difficult to constrain from the available data. Subsequent downbuilding and sediment loading then drove rapid growth of the anticlines, and in one case the differential loading was sufficient to actively pierce the roof (furthest west in Figure 15).

7 Synthesis

As described in Section 6, the geometry, position and orientation of the three main RSBs indicate c. 23.2 km of seaward translation, and up to 32° of rotation; this indicates that related salt structures are now situated a significant distance from where they originated. Figure 17 shows the active salt-related deformation at each time step, as discussed below.

7.1 Albian

The broadly isopachous nature of the Albian indicates: (i) the seabed was broadly flat during its deposition, and thus that the salt had infilled relict, rift-related topography, and broadly thickened seaward; and (ii) regional gravity gliding commenced post-Albian (i.e. the RSBs are strictly post-Albian). However, Albian growth strata indicate that local thin-skinned deformation did occur in at least two areas at this time: (i) at the base of the ramp, in an area of salt and overburden contraction; and (ii) updip, outside of the area of data coverage, where we suggest that early extension drove formation of the somewhat enigmatic, slope-parallel, Set 2 salt rollers (Figure 17a).

7.2 Upper Cretaceous to Eocene

Regional gliding had fully initiated by the end of the Albian, by which time the overburden had thickened and strengthened. This resulted in the development of the first RSB as the salt and overburden were translated over the base-salt ramp (Figure 17b). As the thick salt continued to flow seaward, away from the ramp, accommodation was created adjacent to the ramp, producing landward-thickening and dipping growth packages that onlapped underlying Albian strata. The onset of regional gliding can be attributed to regional tilting of the base-salt driven by thermal subsidence to the SW within the deep basin (Brice et al., 1982; Hudec and Jackson, 2004). The angle necessary to create basin-scale gravitational instability and to thus induce regional gliding can be as little as 1-2° (Peel, 2014).

We suggest the salt-cored anticlines formed at this time at the base of the ramp as the mismatch in salt flux causes deceleration and contraction of the thickening overburden (Dooley et al., 2017). Syn-kinematic sediments accumulated within synclinal depocentres, driving further growth of the anticlines. Updip of the growing salt-cored anticlines, extension continues to dominate the development of the Set 2 structures, creating rafts and turtle structures. Albian rafting has previously been documented elsewhere in the Kwanza Basin (Burollet, 1975; Duval et al., 1992; Lundin, 1992; Mauduit et al., 1997). In these studies the orientation of the early formed rafts was inferred to be parallel to the margin, although they were imaged on 2D seismic lines (i.e. the true relationship between base-salt dip, margin trend, and raft trend was unknown).

7.2.1 Oligocene to Miocene

The Set 1 salt structures are translated away from the base of the ramp and enter an extensional stress field, which transforms the salt-cored anticline into a reactive diapir (Figure 17c). This extension may relate to local acceleration resulting from translation over a steeper part of the base-salt surface, which served to locally increase the rate of seaward salt flow. We argue that local rather than regional stresses drove this change in deformation style, given that the adjacent Set 2 structures enter a phase of contraction at this time.

Whilst structures within Sets 1 and 2 continued to grow during this period due to squeezing and reactive rise, those within Set 3 became inactive and were eventually buried.

7.2.2 Miocene to Recent

The RSBs record an increase in translation rate at this time (from c. 0.2 to 1 mm/yr), despite thinning of the salt (Figure 9). This is attributed to margin uplift during the Miocene, which thereby increased gravitational instability (Lunde et al., 1992; Lundin, 1992; Hudec and Jackson, 2004). Thinning and onlapping of strata across major salt structures indicate that some were tall enough (relative to their overburden thickness) to actively rise and arch their overburden (Figure 17d). Other structures were passively translated and buried as the salt source layer was too thin to feed them. Welds develop and translation rates consequently slowed.

7.2.3 Present

The salt thickness map shows that, at present, most of the study area adjacent to the well-developed salt walls is very close to welding (Figure 5b). This means that there is increased basal drag on the salt, and that seaward translation of salt and overburden is correspondingly slow. The youngest strata still thicken into the youngest RSB, but rather than onlapping its seaward-dipping flank, they thin up onto the ramp, indicating basinward translation persists at a slow rate. This is further supported by the fact that the seabed shows no expression of the RSB, indicating that aggradation keeps up with the rate of displacement. Two salt structures continue to actively rise and thus deform the seabed, but the majority of salt structures are inactive and are being buried (Figure 17e).

8 Discussion

Classic models of salt-influenced passive margins cannot explain the diversity of structural styles and orientations of the salt structures observed in the Outer Kwanza Basin, offshore Angola. Each salt structure set is associated with a unique structural evolution, with many showing evidence for multiple phases of reactivation and inversion. Another key observation is that phases of extension and contraction were synchronous in closely spaced salt structures. This means we cannot appeal to basement-involved shortening as in the Inner Kwanza Basin (Hudec and Jackson, 2002). We suggest this complexity reflects the interaction of seaward salt flow with considerable base-salt topography. A key consequence of this process is that the mid-slope zone of translation, which in classic models is shown to be largely undeformed (Fig. 1a; see Jackson et al., 1994; Schultz-Ela, 2001; Fort et al. 2004; Hudec and Jackson, 2004; Brun and Fort, 2011; Peel, 2014), may in fact be an area of very complex deformation.

Salt deformation on the Angolan margin initiated early in response to gravity gliding but the interaction of salt flow with base-salt topography controlled the subsequent structural evolution, and produced a much more complicated set of salt structures than would typically be associated with salt-influenced passive margins (i.e. margin-parallel structures defining extensional, translational and compressional domains).

Physical models by Dooley et al. (2017) and Dooley et al. (2018) show that the basinward flow of salt and overburden across base-salt relief can generate local extension and contraction anywhere along a margin. Because of this, pre-existing, diapiric and non-diapiric structures can be inverted multiple times as they migrate through these various stress fields. These local stress fields explain how structures from the Kwanza Basin comprise extensional diapirs which are subsequently squeezed during contraction, and folds which evolved into reactive diapirs due to late extension. These structures are very similar to those developed in the multi-ramp models by Dooley et al. (2018), with even greater complexities seen in models with isolated ramps (see their model 5; Fig. 16. These local stress fields also explain how structures experience very different tectonic evolutions, depending on their starting position on the margin and path taken during downdip translation. Consequently, salt structures in the Kwanza Basin have complex evolutionary histories comprising phases of both extension and compression, and different salt structures are associated with different evolutionary histories as they respond to local stresses caused by the underlying topography over which they are translated.

In the Kwanza Basin, steep, seaward-dipping ramps, which change orientation along strike, had the greatest impact on salt-related deformation. Changes in the flux of salt over these ramps generate local stresses that deform the salt and its overburden. Convex- and concave-into-the-basin segments of the ramps may have also initiated locally divergent and convergent gliding (Cobbold and Szatmari, 1991; Tadeu dos Reis et al., 2008). The effect of these local stresses on overburden deformation depends on the thickness of the latter, and the presence and orientation of any pre-existing weaknesses (e.g. precursor diapirs).

Unlike the strike-elongate, broadly linear base-salt ramps, the more isolated, sub-circular base-salt highs are not obviously associated with any salt structures or specific style of overburden deformation. The reason for this is not yet clear, although this observation may suggest there is a critical ratio between salt thickness and relief height; i.e. a threshold value must be reached before stresses induced at the base of the salt are transferred into the overburden. Or put another way, low-relief features only produce stress perturbations sufficient to deform the overburden when the salt is very thin. An alternative interpretation for the apparent lack of structures above isolated base-salt highs is that any structures that did form have since been translated out of the study area or overprinted by later deformation. Other controls on the structural evolution of the salt and overburden which require further study include: sedimentation rate and distribution, the composition and rheology of both the salt (i.e. in case where the salt is mechanically layered; e.g. Van Gent et al., 2010; Fiduk and Rowan, 2012; Jackson et al., 2014, 2015) and overburden, and the role of active basement-involved tectonics.

This study concludes that, in this area downdip translation over base-salt topography played a key role in the structural evolution of the salt walls. The diversity of salt wall orientations and structural styles in the Kwanza Basin demonstrates the significant impact which salt flow over base-salt topography can have on the structural evolution of the basin. We suggest that the effects of base-salt relief in the Kwanza Basin are important because the ratio of base-salt relief to depositional salt thickness is high. Only when this ratio is low (e.g. for a smooth base-salt surface) may simple models of gravity gliding and spreading accurately capture the origin and evolution of salt structures on a margin.

9 Conclusions

We used 3D seismic data to reconstruct the tectono-stratigraphic evolution of the Outer Kwanza Basin, with the aim being to investigate how the interaction of salt flow with base-salt relief influenced the origin and growth of salt structures on the margin. The key conclusions of our study are:

- Ramp-syncline basins record a minimum of 23 km of translation and 32 degrees of rotation in the mid-slope domain of the Outer Kwanza Basin
- Clockwise direction of rotation suggests increasing velocities, and therefore increasing salt thickness, to the south
- Salt tectonics in the Kwanza Basin is characterised by advanced diapiric salt structures. The salt structures can be divided broadly into three sets characterised by their orientations and structural styles.
- The stratigraphic relationships in the overburden indicate that the evolutionary history of each set is unique and cannot be explained in terms of conventional models of gravity gliding and gravity spreading on salt-influenced passive margins.
- The effects of salt flow over base-salt relief played a crucial role in the development of the salt structures. The local variations in salt flux cause local compression or extension, thereby fundamentally controlling the spatial distribution, orientation and structural style of the salt structures.

10 References

Bally, A.W., 1981. Thoughts on the tectonics of folded belts. Geological Society, London, Special Publications, 9(1), pp.13-32.

Brice, S.E., Cochran, M.D., Pardo, G. and Edwards, A.D., 1982. Tectonics and Sedimentation of the South Atlantic Rift Sequence: Cabinda, Angola: Rifted Margins: Field Investigations of Margin Structure and Stratigraphy.

Brink, A.H., 1974. Petroleum geology of Gabon basin. AAPG Bulletin, 58(2), pp.216-235.

Brown, A.R., 2011. Interpretation of three-dimensional seismic data. Society of Exploration Geophysicists and American Association of Petroleum Geologists.

Brun, J.P. and Fort, X., 2011. Salt tectonics at passive margins: Geology versus models. Marine and Petroleum Geology, 28(6), pp.1123-1145.

Burollet, P.F., 1975. Tectonique en radeaux en Angola. Bulletin de la Société géologique de France, 7(4), pp.503-504.

Cobbold, P.R. and Szatmari, P., 1991. Radial gravitational gliding on passive margins. Tectonophysics, 188(3-4), pp.249-289.

Dooley, T.P. and Hudec, M.R., 2017. The effects of base-salt relief on salt flow and suprasalt deformation patterns—Part 2: Application to the eastern Gulf of Mexico. Interpretation, 5(1), pp.SD25-SD38.

Dooley, T.P., Hudec, M.R., Carruthers, D., Jackson, M.P. and Luo, G., 2017. The effects of base-salt relief on salt flow and suprasalt deformation patterns—Part 1: Flow across simple steps in the base of salt. Interpretation, 5(1), pp.SD1-SD23.

Dooley, T.P., Hudec, M.R., Pichel, L.M. and Jackson, M.P., 2018. The impact of base-salt relief on salt flow and suprasalt deformation patterns at the autochthonous, paraautochthonous and allochthonous level: insights from physical models. Geological Society, London, Special Publications, 476, pp.SP476-13.

Duffy, O.B., Dooley, T.P., Hudec, M.R., Jackson, M.P., Fernandez, N., Jackson, C.A. and Soto, J.I., 2018. Structural evolution of salt-influenced fold-and-thrust belts: a synthesis and new insights from basins containing isolated salt diapirs. *Journal of Structural Geology*, *114*, pp.206-221.

Duval, B., Cramez, C. and Jackson, M.P.A., 1992. Raft tectonics in the Kwanza basin, Angola. Marine and Petroleum Geology, 9(4), pp.389-404.

Evans, R., 1978. Origin and significance of evaporites in basins around Atlantic margin. AAPG Bulletin, 62(2), pp.223-234.

Fort, X., Brun, J.P. and Chauvel, F., 2004. Contraction induced by block rotation above salt (Angolan margin). Marine and Petroleum Geology, 21(10), pp.1281-1294.

Gaullier, V., Brun, J.P., Gue, G. and Lecanu, H., 1993. Raft tectonics: the effects of residual topography below a salt decollement. Tectonophysics, 228(3-4), pp.363-381.

Hudec, M.R. and Jackson, M.P., 2002. Structural segmentation, inversion, and salt tectonics on a passive margin: Evolution of the Inner Kwanza Basin, Angola. Geological Society of America Bulletin, 114(10), pp.1222-1244.

Hudec, M.R. and Jackson, M.P., 2004. Regional restoration across the Kwanza Basin, Angola: Salt tectonics triggered by repeated uplift of a metastable passive margin. AAPG bulletin, 88(7), pp.971-990.

Hudec, M.R., Norton, I.O., Jackson, M.P. and Peel, F.J., 2013. Jurassic evolution of the Gulf of Mexico salt basin. AAPG bulletin, 97(10), pp.1683-1710.

Jackson, M.P. and Hudec, M.R., 2005. Stratigraphic record of translation down ramps in a passive-margin salt detachment. Journal of Structural Geology, 27(5), pp.889-911.

Jackson, M.P. and Hudec, M.R., 2017. Salt tectonics: Principles and practice. Cambridge University Press.

Jackson, M.P., Hudec, M.R., Fraenkl, R., Sikkema, W., Binga, L. and Da Silva, J., 2001. Minibasins translating down a basement ramp in the deepwater monocline province of the Kwanza Basin, Angola [abs.]. In American Association of Petroleum Geologists Annual Meeting Official Program (Vol. 10, p. A99).

Jackson, M.P., Vendeville, B.C. and Schultz-Ela, D.D., 1994. Structural dynamics of salt systems. Annual Review of Earth and Planetary Sciences, 22(1), pp.93-117.

Lunde, G., Aubert, K., Lauritzen, O. and Lorange, E., 1992. Tertiary uplift of the Kwanza Basin in Angola. Géologie Africaine: Coll. Géol. Libreville, Recueil des Communications. Elf Aquitaine, Boussens, France, pp.99-117.

Lundin, E.R., 1992. Thin-skinned extensional tectonics on a salt detachment, northern Kwanza Basin, Angola. Marine and Petroleum Geology, 9(4), pp.405-411.

Marton, L.G., Tari, G.C. and Lehmann, C.T., 2000. Evolution of the Angolan passive margin, West Africa, with emphasis on post-salt structural styles. Geophysical Monograph-American Geophysical Union, 115, pp.129-150.

Mauduit, T., Guerin, G., Brun, J.P. and Lecanu, H., 1997. Raft tectonics: the effects of basal slope angle and sedimentation rate on progressive extension. Journal of Structural Geology, 19(9), pp.1219-1230.

Peel, F.J., 2014. The engines of gravity-driven movement on passive margins: Quantifying the relative contribution of spreading vs. gravity sliding mechanisms. Tectonophysics, 633, pp.126-142.

Peel, F., Jackson, M. and Ormerod, D., 1998. Influence of major steps in the base of salt on the structural style of overlying thin-skinned structures in deep water Angola. In American Association of Petroleum Geologists International Conference and Exhibition, Rio de Janeiro, Brazil, November, Extended Abstracts Volume (pp. 366-367).

Pichel, L.M., Peel, F., Jackson, C.A. and Huuse, M., 2018. Geometry and kinematics of salt-detached ramp syncline basins. Journal of Structural Geology, 115, pp.208-230.

Pichel, L.M., Jackson, C.A.L., Peel, F. and Dooley, T.P., 2019. Base-Salt Relief Controls on Salt-Tectonic Structural Style, São Paulo Plateau, Santos Basin, Brazil. Basin Research.

Price, N.J. and Cosgrove, J.W., 1990. Analysis of geological structures. Cambridge University Press.

Quirk, D.G., Schødt, N., Lassen, B., Ings, S.J., Hsu, D., Hirsch, K.K. and Von Nicolai, C., 2012. Salt tectonics on passive margins: examples from Santos, Campos and Kwanza basins. Geological Society, London, Special Publications, 363(1), pp.207-244.

Rowan, M.G., Peel, F.J., Vendeville, B.C. and Gaullier, V., 2012. Salt tectonics at passive margins: Geology versus models–Discussion. Marine and Petroleum Geology, 37(1), pp.184-194.

Schultz-Ela, D.D., 2001. Excursus on gravity gliding and gravity spreading. Journal of Structural Geology, 23(5), pp.725-731.

Spathopoulos, F., 1996. An insight on salt tectonics in the Angola Basin, South Atlantic. Geological Society, London, Special Publications, 100(1), pp.153-174.

Tadeu dos Reis, A., Gorini, C., Weibull, W., Perovano, R., Mepen, M. and Ferreira, É., 2008. Radial gravitational gliding indicated by subsalt relief and salt-related structures: the example of the Gulf of Lions, western Mediterranean. Revista Brasileira de Geofísica, 26(3), pp.347-365.

Vendeville, B.C. and Jackson, M.P., 1992a. The rise of diapirs during thin-skinned extension. Marine and Petroleum Geology, 9(4), pp.331-354.

Vendeville, B.C. and Jackson, M.P.A., 1992b. The fall of diapirs during thin-skinned extension. Marine and Petroleum Geology, 9(4), pp.354-371.

von Nicolai, C., 2011. The Interplay of Salt Movements and Regional Tectonics at the Passive Continental Margin of the South Atlantic, Kwanza Basin. Unpublished PhD thesis. Universität Potsdam. [https://goo.gl/8LwQBY]

Weijermars, R., Jackson, M.T. and Vendeville, B., 1993. Rheological and tectonic modeling of salt provinces. Tectonophysics, 217(1-2), pp.143-174.

11 Tables

	Time (Ma)	Displacement (km)	Rotation (deg)	Translation rate (mm/yr)	Rotation rate (deg/Myr)
	100.5	0	0		
RSB 1	33.9	11.9	20	0.18	0.30
RSB 2	5.3	17.8	27	0.21	0.24
RSB 3	0	23.2	32	1.0	0.90

Table 1: Translation and rotation of ramp syncline basins

12 Figures

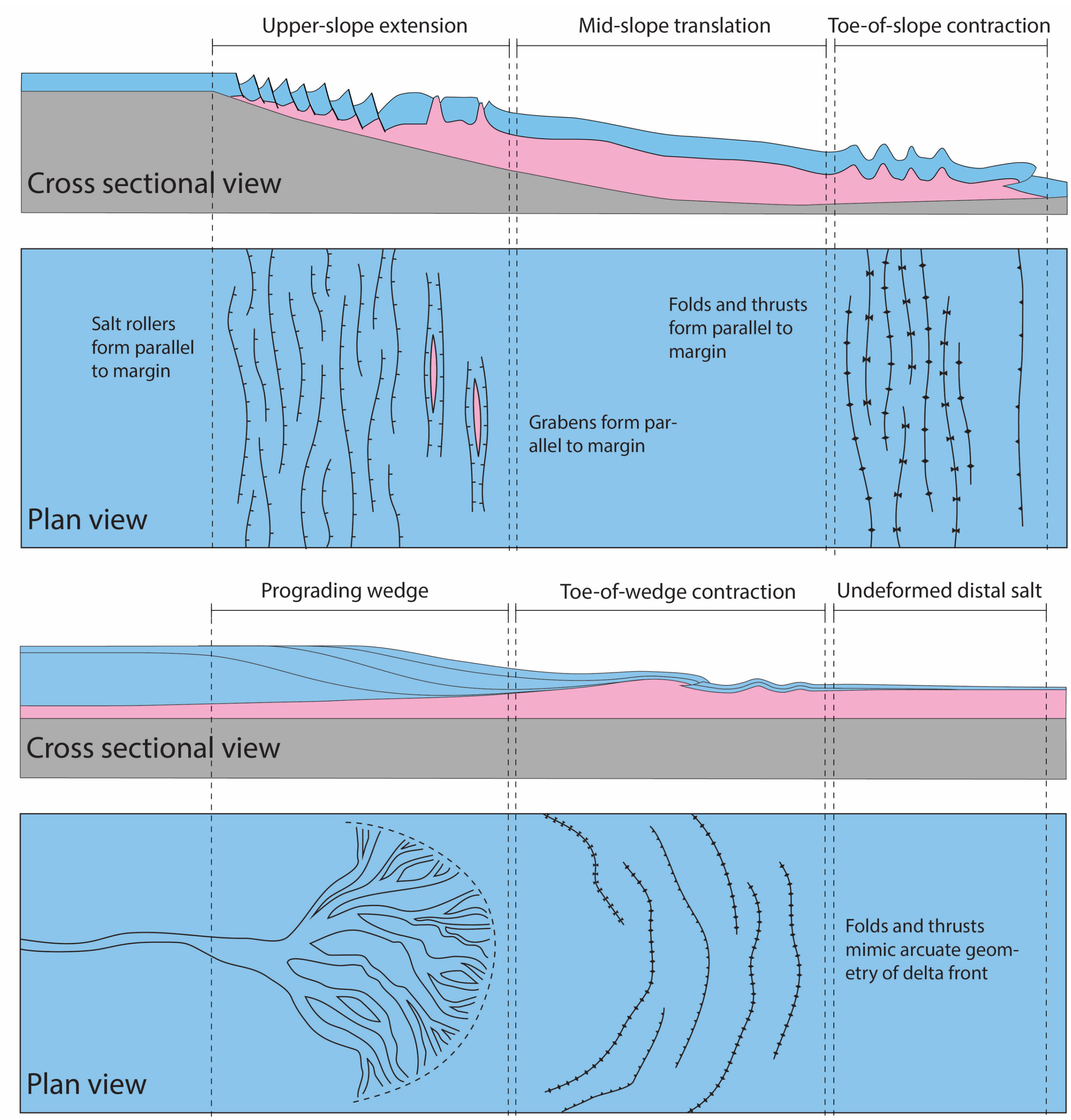

Figure 1: Cross sectional and plan view schematic diagrams of end member models of salt tectonic systems: a) gravity gliding, and b) gravity spreading, showing the types of structures and orientations associated with each kinematic domain.

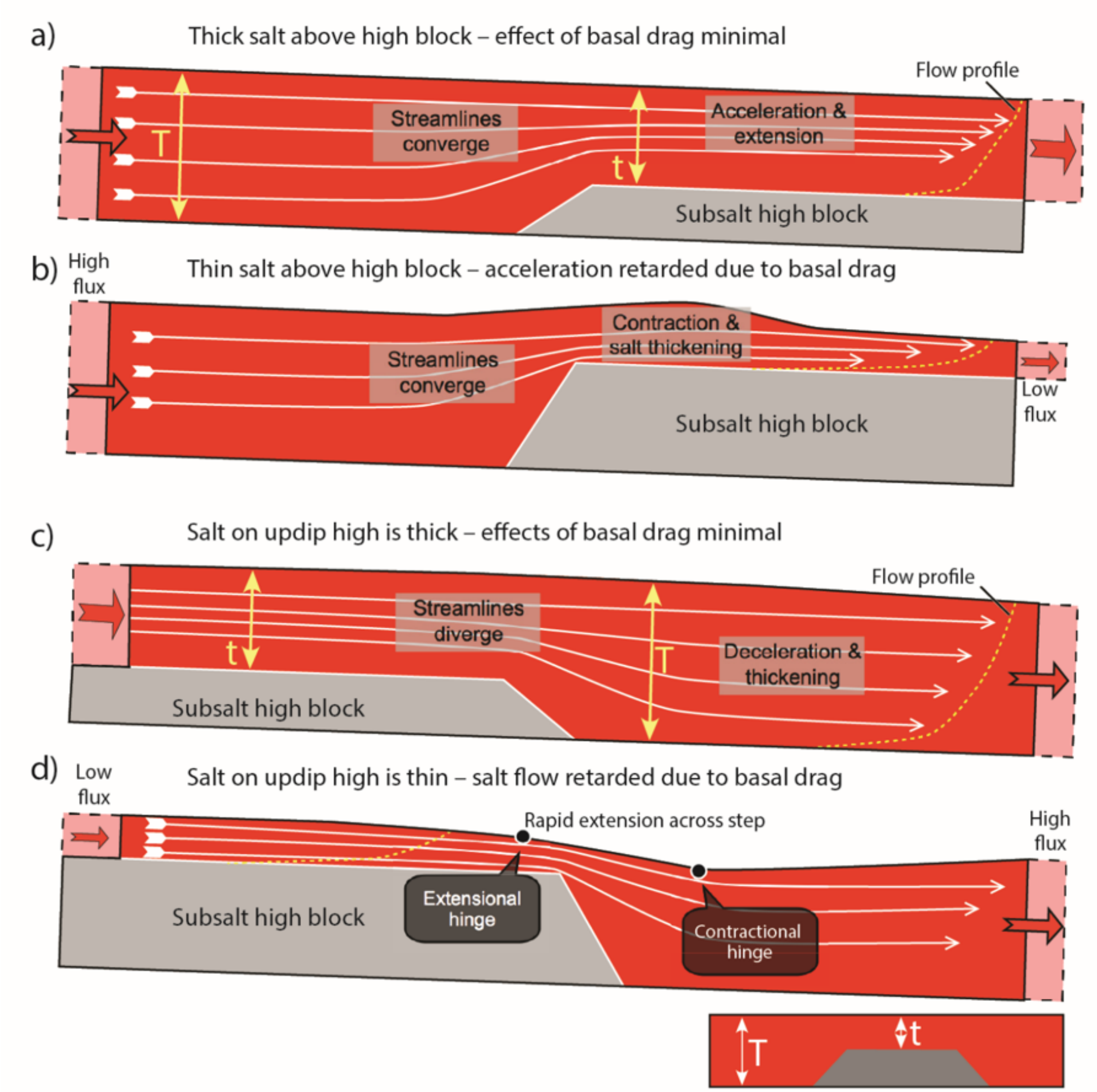

Figure 2: Synoptic diagram showing the complex interaction of base-salt relief with salt flow, as determined from physical models. Base-salt relief causes local acceleration and deceleration which in turn causes local extensional and contractional stress fields. The effect on salt flow is different for thick salt cases, a) and c), compared to thin salt cases, b) and d) respectively. Note that these stress fields may also vary through time. From Dooley et al. (2017).

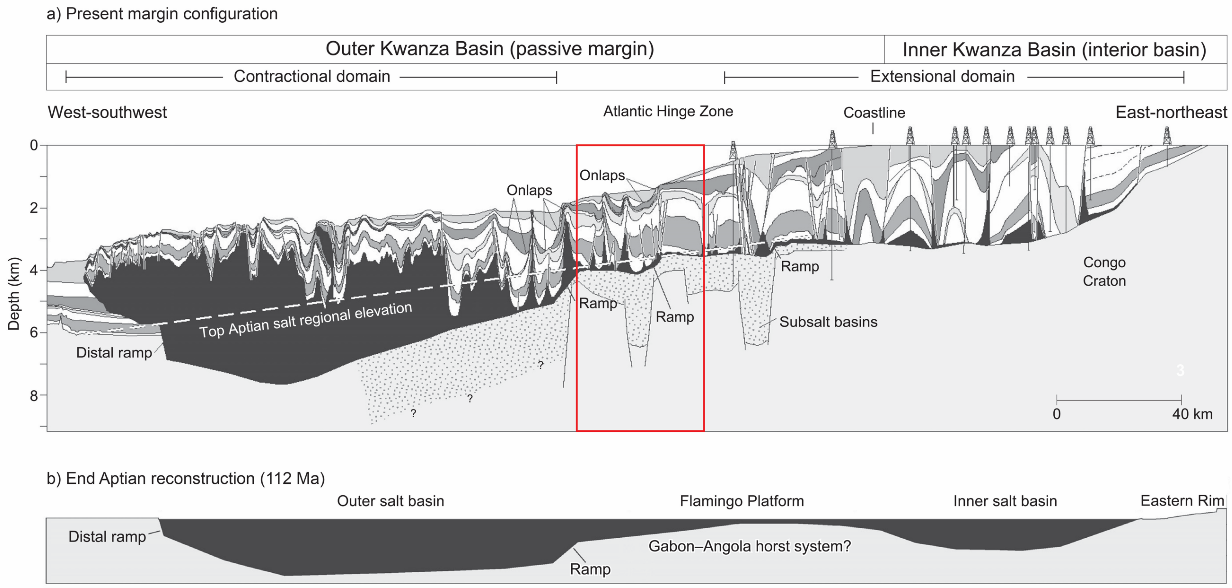

Figure 3: a) Regional line showing present day configuration of the Angolan margin from shelf to distal salt nappe. Note the presence of several ramps on the base-salt surface. Location of line shown in Figure 4. Red box highlights approximate position of dataset used in this study. b) End Aptian reconstruction showing initial division of Inner and Outer salt basins. Modified from Hudec and Jackson (2004).

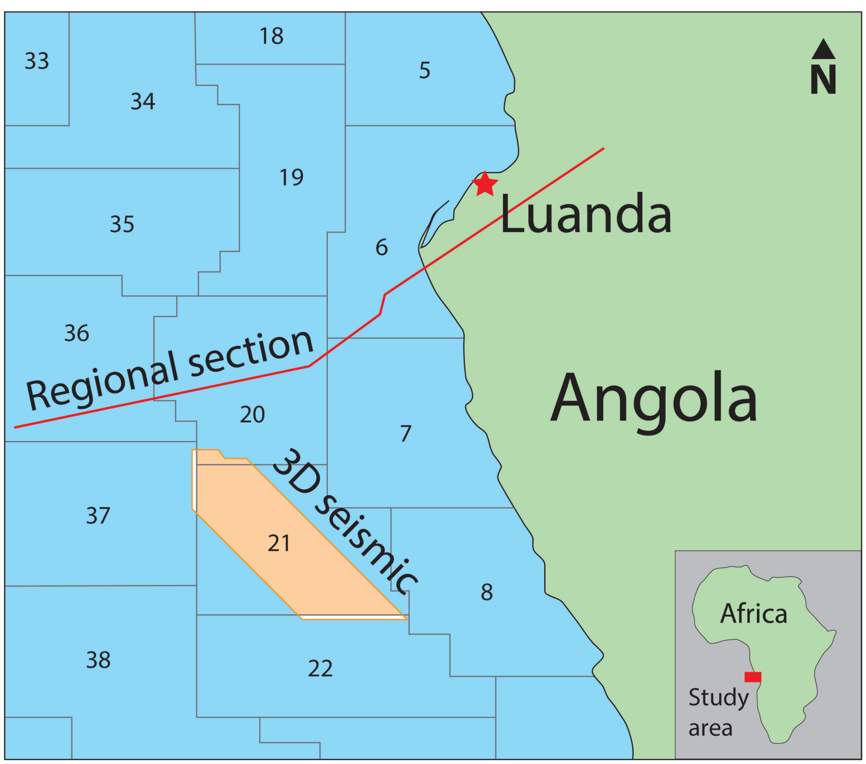

Figure 4: Regional map showing location of 3D dataset used in this study (orange) and regional line (see Figure 3). Dataset covers Licensing Block 21 of the offshore Angolan margin.

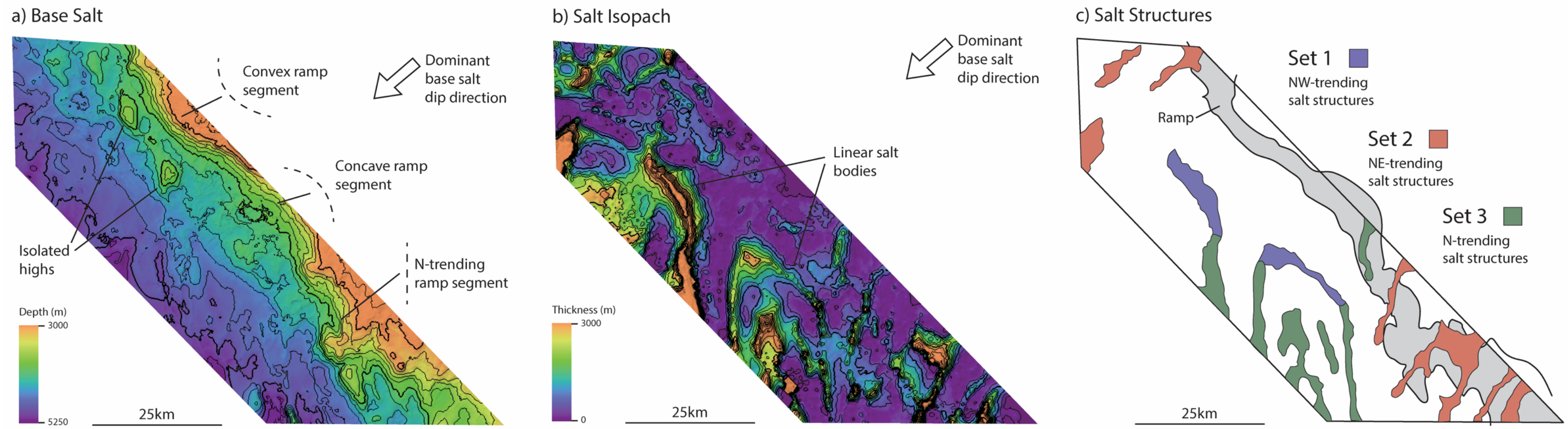

Figure 5: a) Depth map of base-salt surface showing dominant dip to the SW. Ramp runs across updip edge of the dataset, broadly sub-parallel to margin but with variable geometry along strike. b) Salt isopach map. Areas of increased thickness correspond to location of salt structures. Areas of minimal thickness show where salt is close to welding. c) Schematic distribution of salt structures across the study area, dividing the structures into three broad sets characterised by their orientation and structural style. Shaded area shows location of base-salt ramp. Seismic data supplied by CGG.

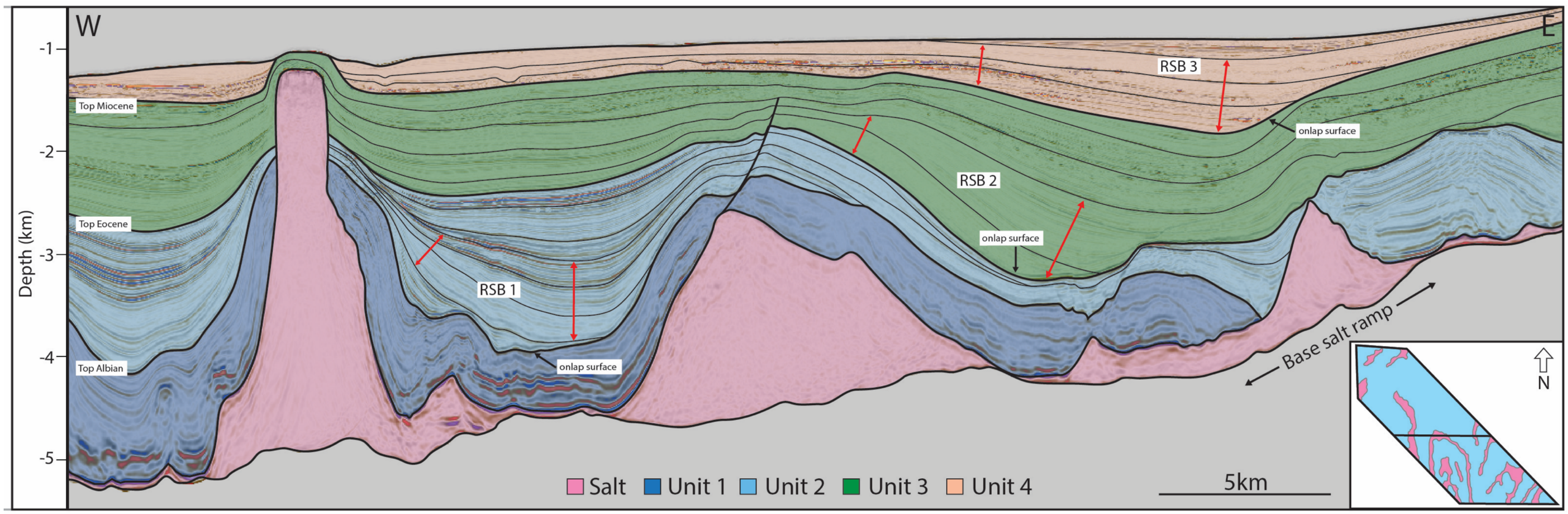

Figure 6: Representative seismic geosection showing series of salt structures (see inset map for location). Key interpreted units in the overburden (1-4) and approximate ages of key surfaces (Top Albian, Top Eocene, Top Miocene). Stacked ramp syncline basins (RSB1, RSB2, RSB3) and location of updip base-salt ramp. Seismic data supplied by CGG.

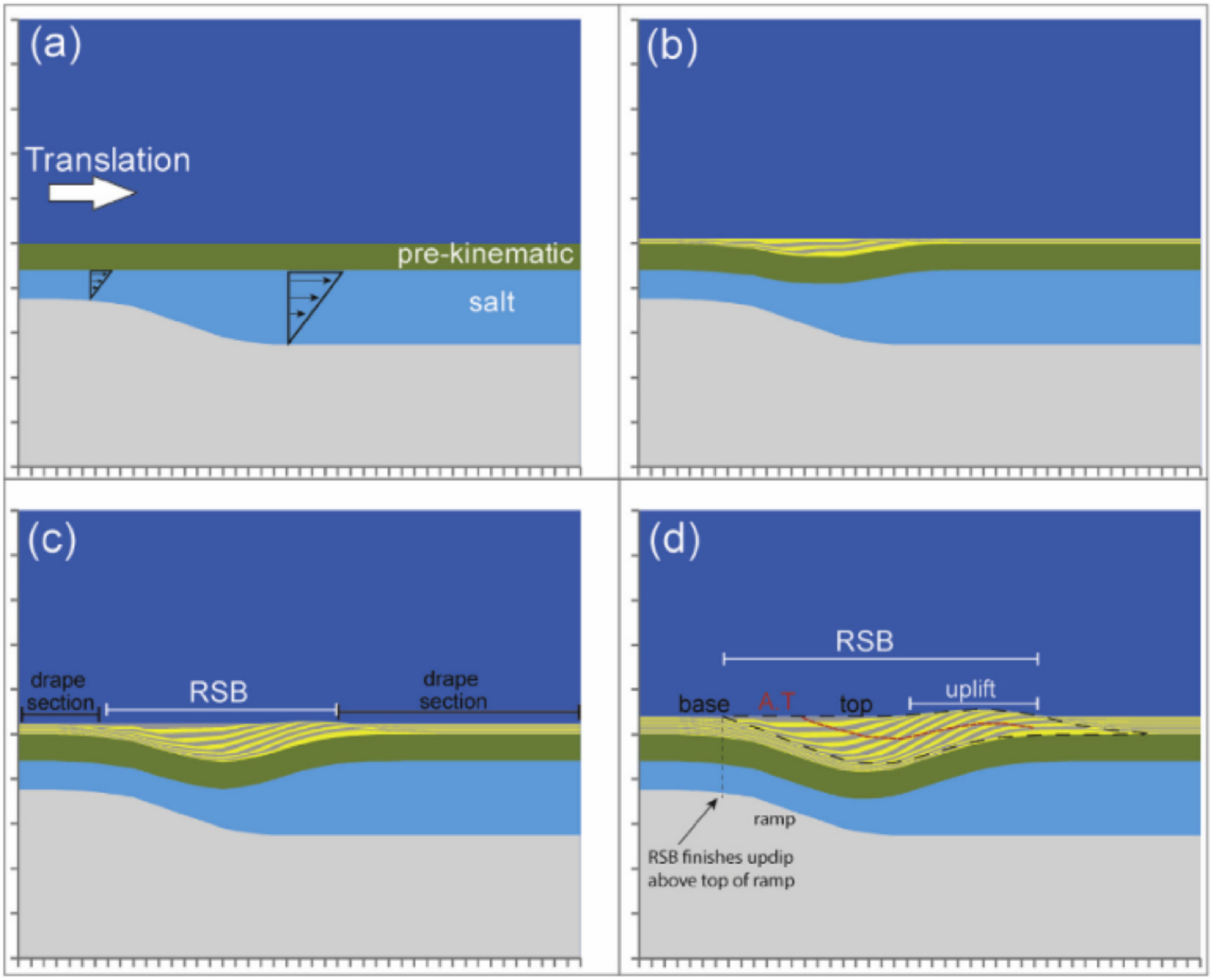

Figure 7: Numerical model showing incremental development of ramp syncline basin during basinward translation. a) Isopachous pre-kinematic strata prior to translation. b) Imbalance of salt flux creates accommodation space above ramp which fills which growth strata thickening into ramp. c) Early growth strata are rotated and moved downdip as translation continues. d) Fully developed ramp syncline basin showing monoclinal geometry of growth strata, basal onlap surface and distal uplift. From Pichel et al. (2018).

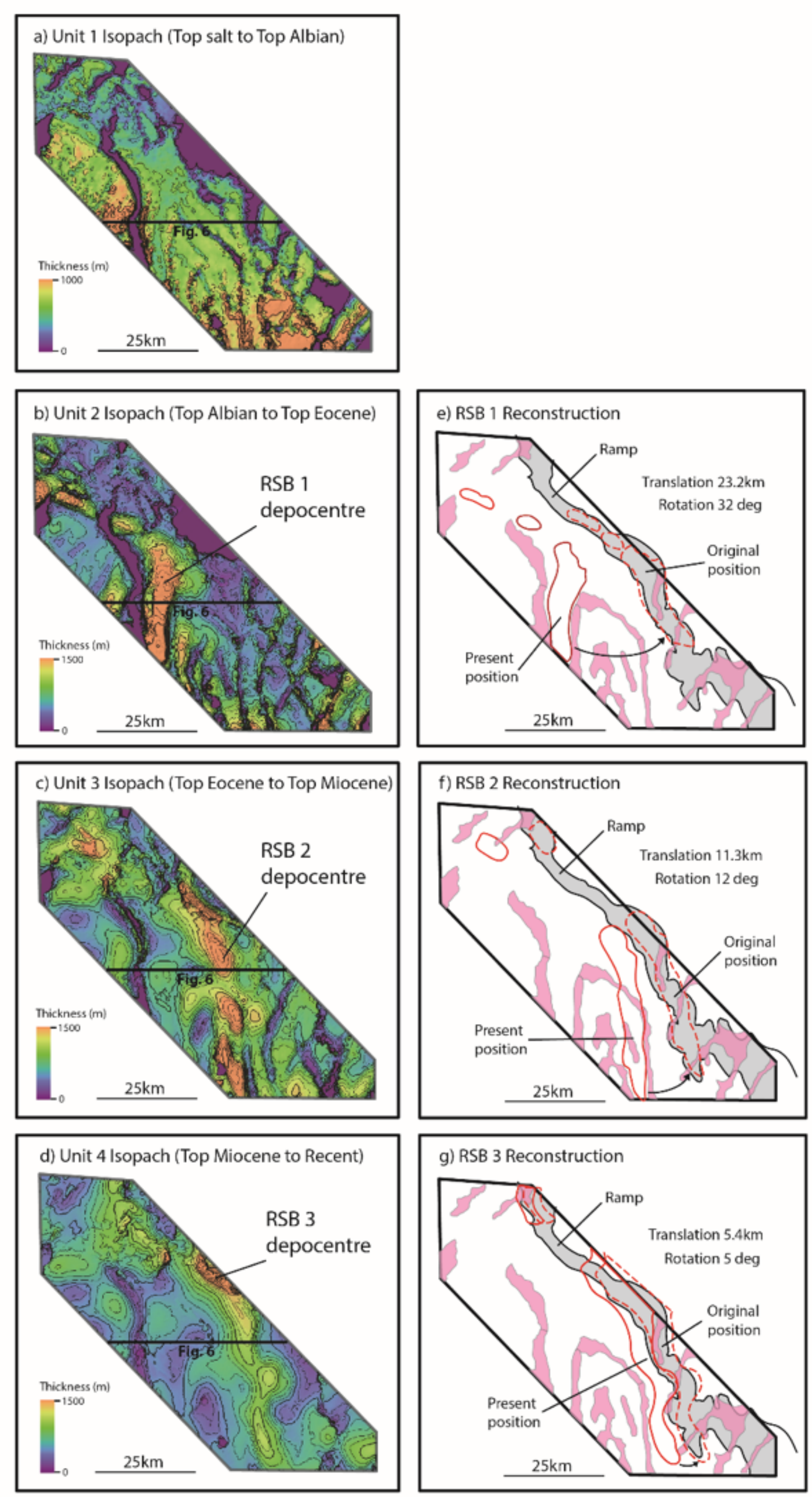

Figure 8: a-d) Isopach maps for key units (see Figure 6). Thick, linear depocentres correspond to ramp syncline basins. Location of Figure 6 section is shown for reference. e-g) Reconstructed positions of ramp syncline basins above the causal base-salt ramp, allowing translation and rotation to be quantified through time. Seismic data supplied by CGG.

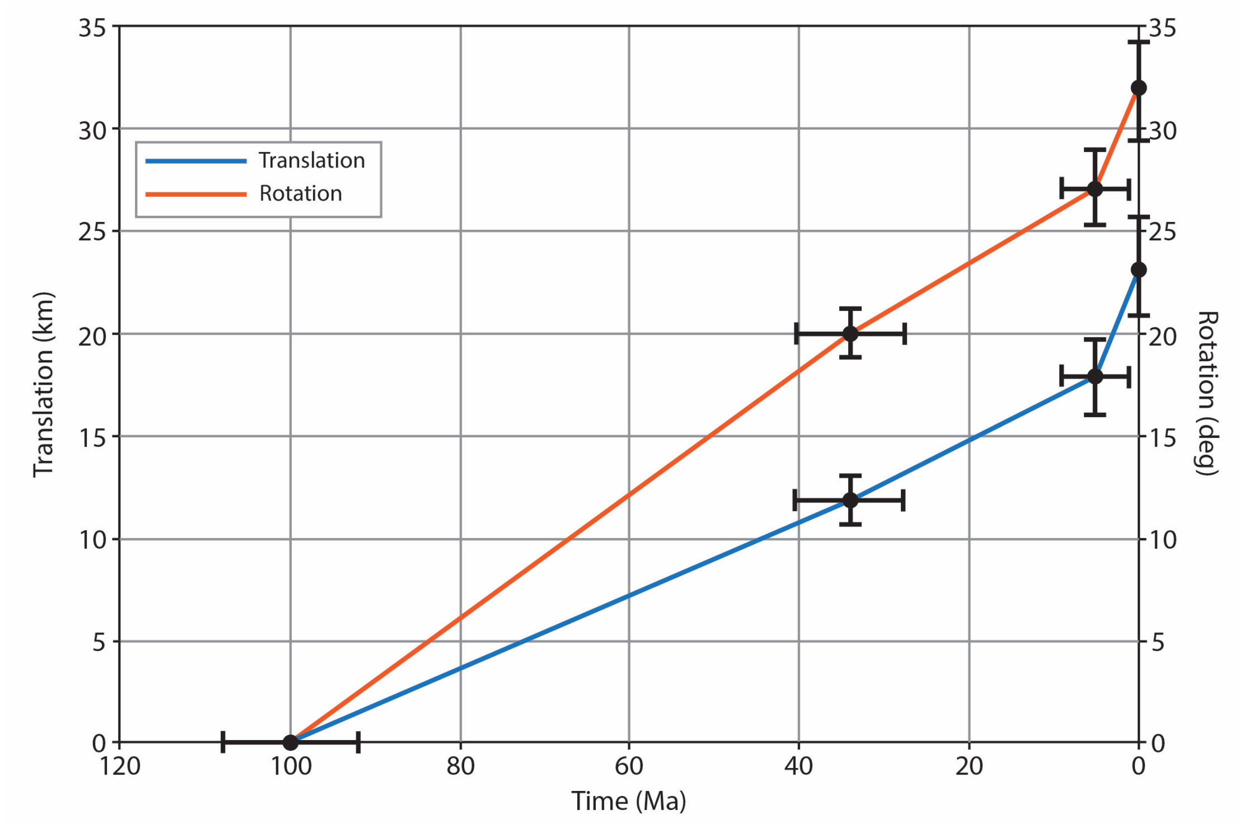

Figure 9: Graph showing translation and rotation through time since end Albian, as derived from ramp syncline basins (see Table 1).

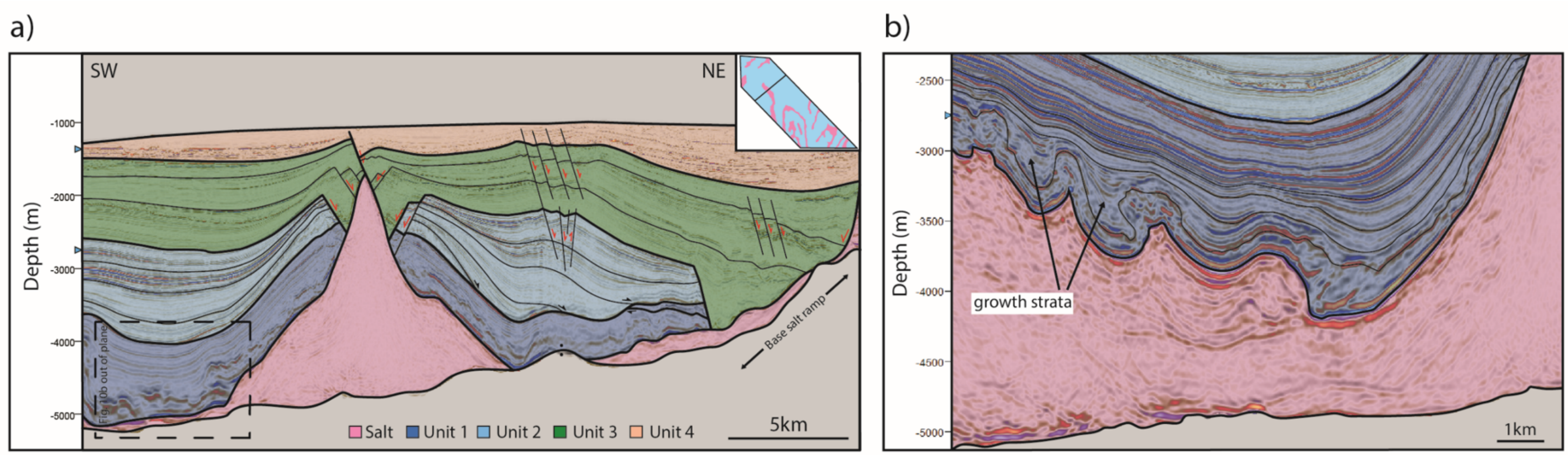

Figure 10: a) Seismic geosection through Set 1 salt wall (see inset map for location). Note the triangular geometry, inward-dipping crestal normal faults and updip base-salt ramp. b) Enlarged section showing buckle folds and growth strata on the flank of the salt wall at base of Unit 1 (out of plane of section shown in Figure 10a). Seismic data supplied by CGG.

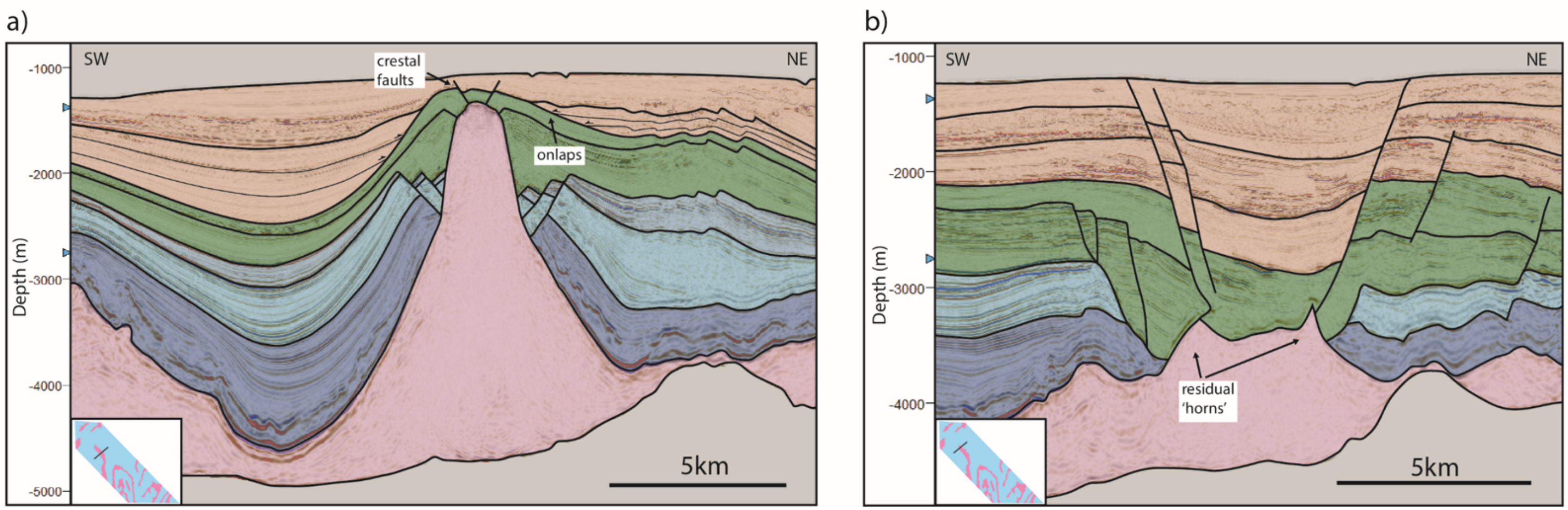

748 Figure 11 - a) Seismic geosecton through central Set 1 salt wall showing characteristics indicative of active rise. b) Seismic geosection through end of Set 1 salt wall showing characteristics indicative of diapir collapse. Locations shown in inset maps. Seismic data supplied by CGG.

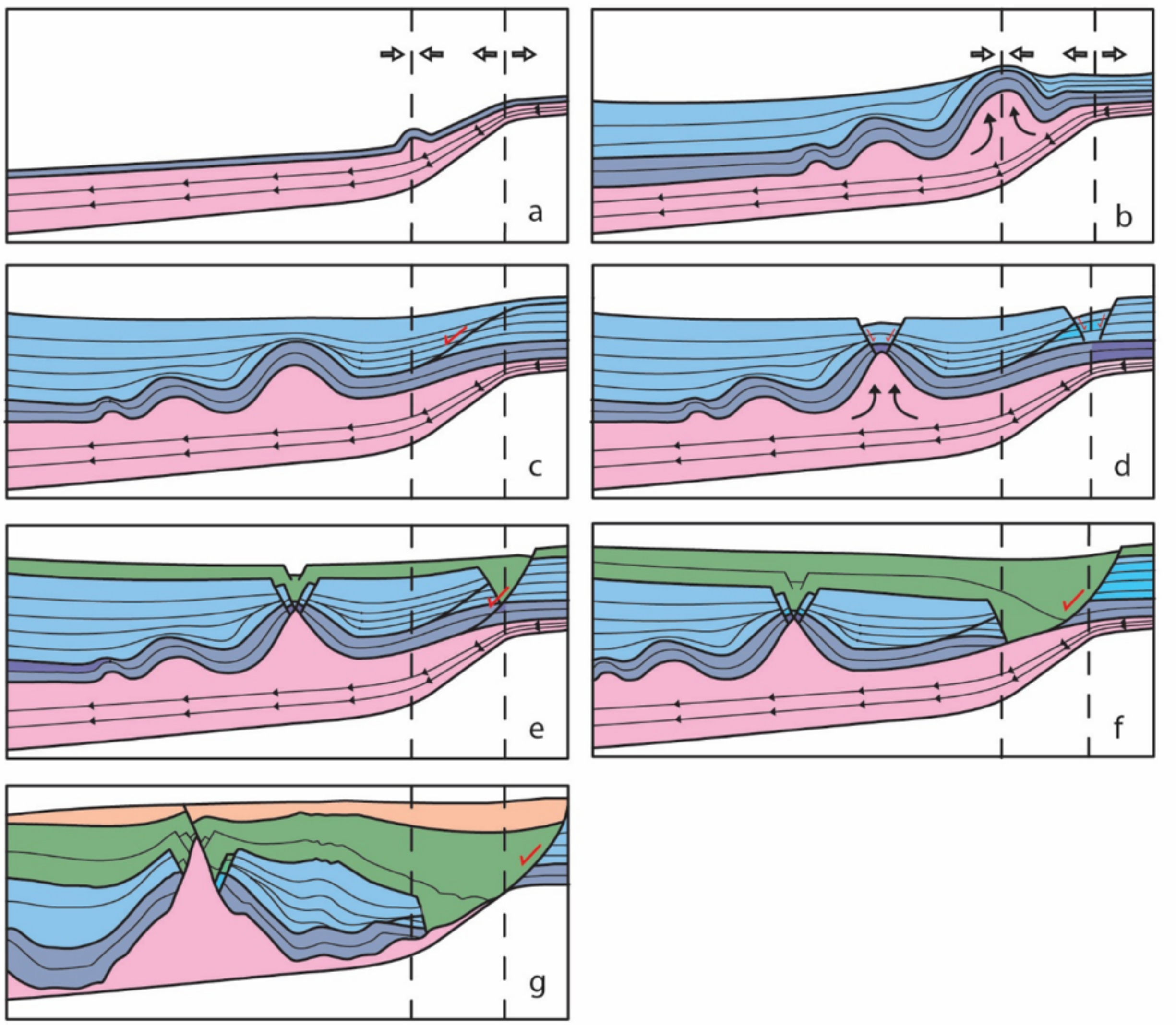

Figure 12: Schematic evolution of the Set 1 salt structures. Location of each schematic time step shown in Figure 17. a) Initial contraction as salt decelerates at base of ramp. b) Overburden thickening and sediment loading drives growth of salt-cored anticline as translation continue. c) Overburden strengthens and normal fault develops above ramp. d) Local extension as grabens open at points of overburden weakness – top of the ramp and crest of the salt-cored anticline. e) Syn-kinematic sediments thicken over crest as reactive rise drives further growth of salt wall. Normal fault above ramp grows and detaches into salt. f) Normal fault facilitates continued downdip translation of the salt and overburden. e) Present day geometry.

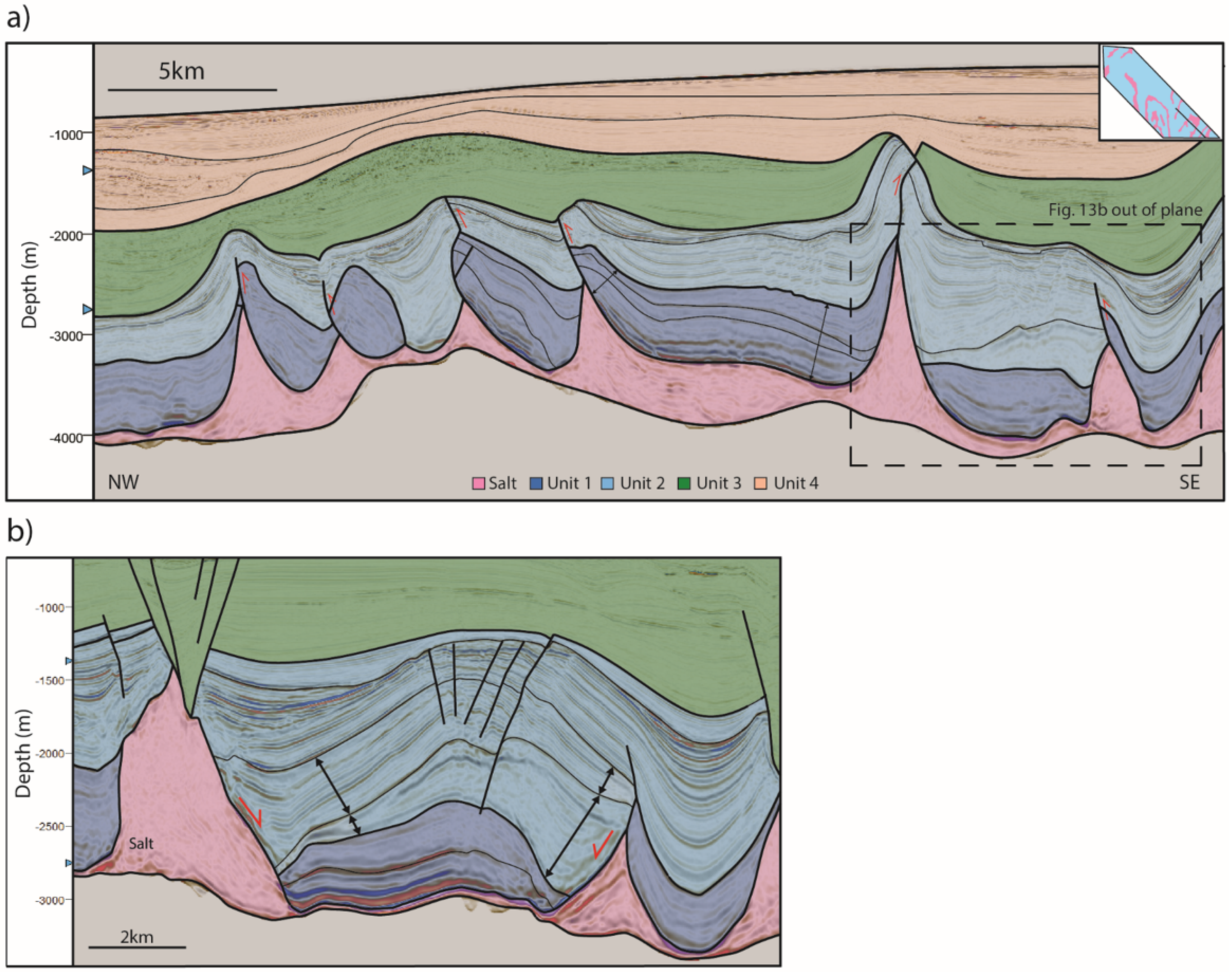

Figure 13: a) Seismic geosection through Set 2 salt structures (see inset map for location; note that as this section is taken perpendicular to the Set 2 salt walls, the net flow direction of salt is out of the page, towards the viewer). Note the rafts of Unit 1 and the thrust faults associated with each salt wall. b) Enlarged section showing turtle anticline structure (out of plane of section shown in Figure 13a). Seismic data supplied by CGG.

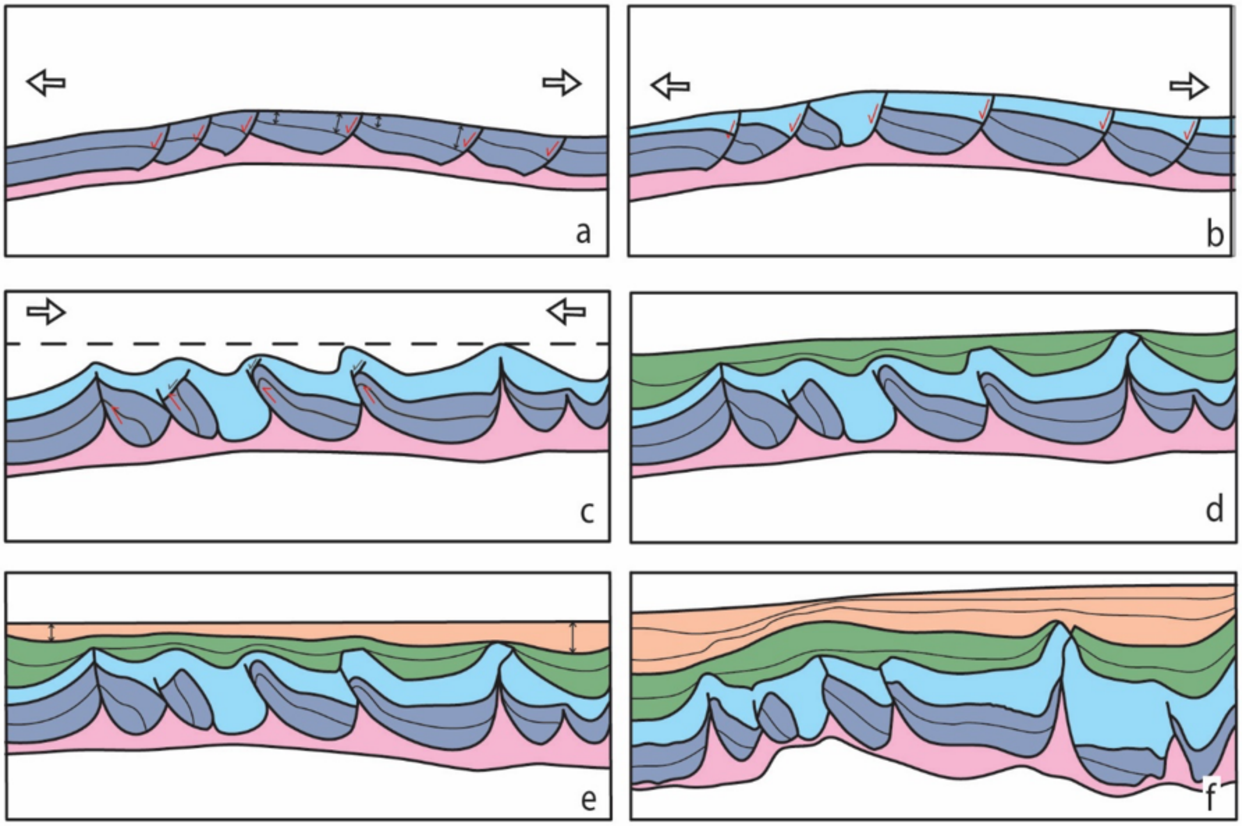

Figure 14: Schematic evolution of the Set 2 salt structures. Locations of each schematic time step shown in Figure 17. a) Early development of extensional salt rollers and associated growth strata. Normal faults detach in salt and dip to the west. b) Continued extension leads to rafting (turtle anticline develops out of plane). c) Onset of contraction exploiting weak salt rollers and causing rafts to thrust over each other. Local erosion of uplifted strata. d) Sediments onlap residual highs and salt walls become buried. e) Inactivity of salt structures and continued burial. Growth strata shows asymmetric subsidence as downdip translation progresses. f) Present day geometry.

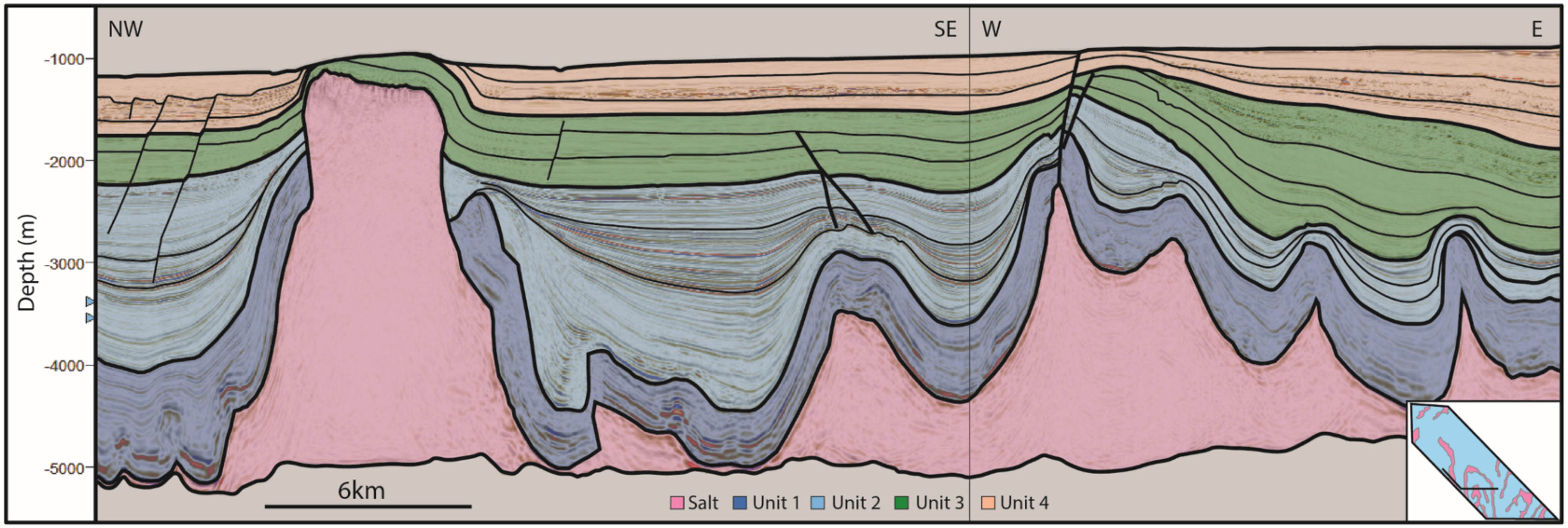

Figure 15: Seismic geosection through Set 3 salt structures (see inset map for location; note that line bends in order to cross a larger Set 3 salt wall, the only one to pierce the overburden). Note the isopachous nature of Unit 1 and prominent growth strata of Unit 2. Seismic data supplied by CGG.

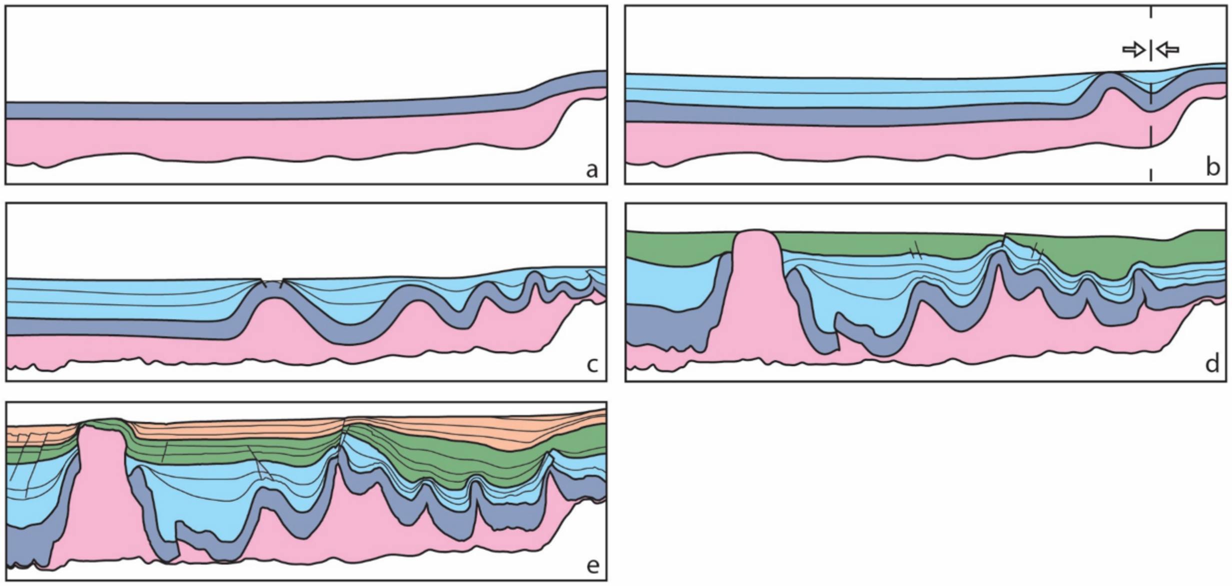

Figure 16: Schematic evolution of the Set 3 salt structures. Locations of each schematic time step shown in Figure 17. a) Pre-kinematic, isopachous deposition of Unit 1. b) Rapid growth of salt-cored anticlines. c) Salt-cored anticlines translated away from base-salt ramp and amplified by sediment loading. New ones develop in their place. d) Growth of anticlines slows and most become buried. The buoyancy associated with the oldest and largest anticline is enough to generate active rise and pierce the overburden. e) Present day geometry.

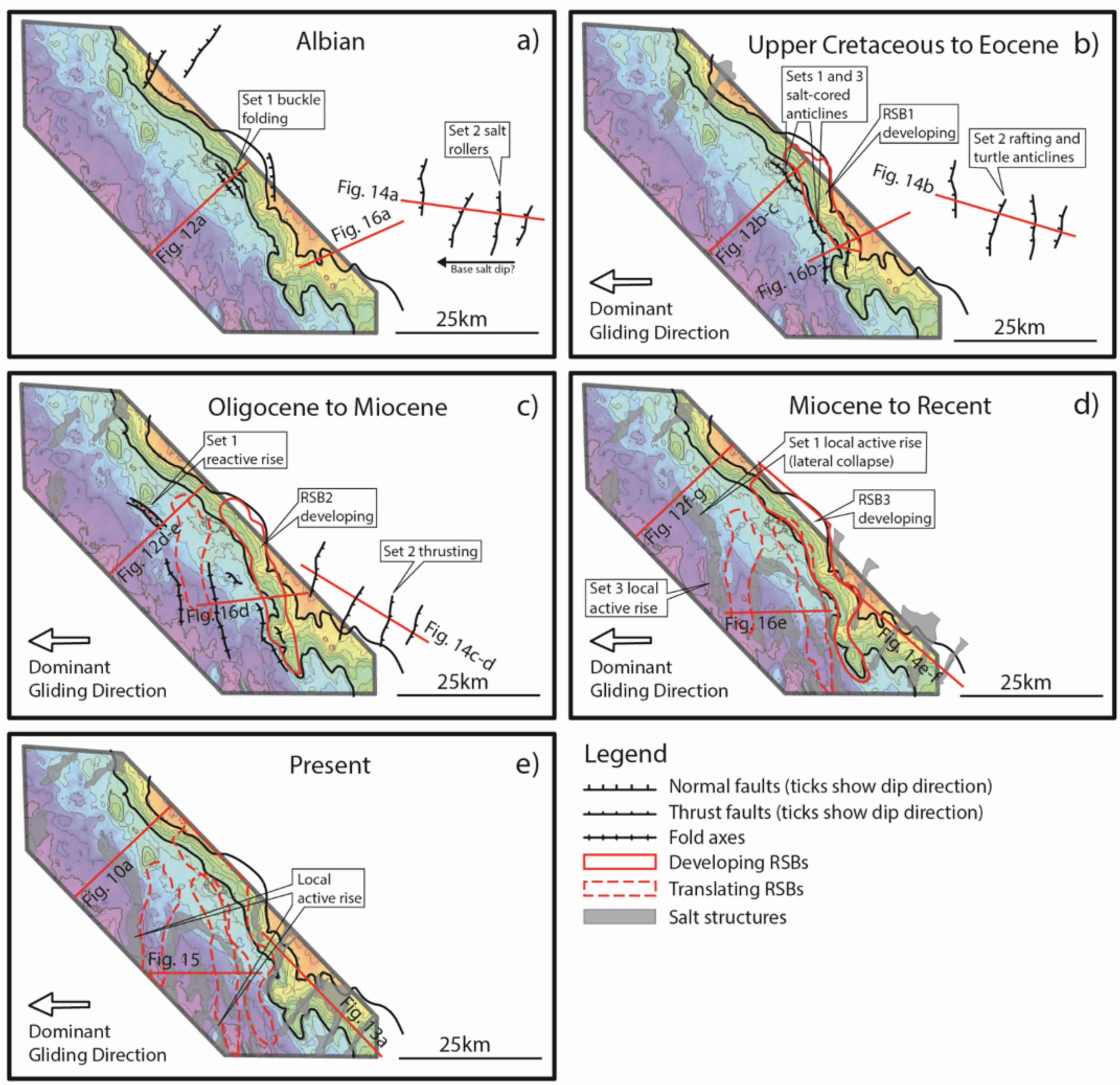

Figure 17: Reconstructed salt structure evolution through time using reconstructed positions of ramp syncline basins (see Figure 8). Shows active structures and development of RSBs at each time step, overlaid on map of base-salt relief. See Figures 12, 14 and 16 for schematic structural evolutions.